Chapter 4

Thermal model fits to thermal infrared data and derivation of albedos and diameters

4.1 Foreword

In order to derive sizes and albedos of the NEAs, the STM, the FRM and the NEATM were fitted to the measured infrared fluxes. Thermal-model fitting and results of the observations carried out at Keck are discussed by Delbó et al. (2003). However, three more NEAs for which apparently we had no detection, could have been detected in LWS frames by accurate registration of the nod-sets. In this chapter, we comment mainly on the derivation of diameters and albedos from the thermal infrared observations obtained at the ESO and at the NASA-IRTF. A summary of radiometric results is presented at the end of this chapter.

4.2 Introduction

In order to derive sizes (in terms of effective diameter, i.e. the diameter of the sphere of equivalent projected area) and geometric albedos p_V, the STM the FRM and the NEATM were fitted to the measured infrared fluxes. For more detailed discussions of the three thermal models see Chapter 2 of this work. An assessment of the modeling error is usually very difficult. Application of the three thermal models gives idea of the modeling uncertainties involved. However, on the basis of the analysis of the radiometrically derived diameters and albedo from this set of observations and with the help of the thermophysical model developed in Chapter 6, we have estimated, in section 6.9, the modeling uncertainties inherent in the use of the STM and the NEATM.

In a number of cases in which the data are of poor quality, or observations were made over a small wavelength range, the NEATM fits and the resulting η-values are not well constrained. In these cases default values of η were used. Harris (1998) has shown that a value of 1.2 produces NEA diameters in good agreement with radar results and albedos consistent with the values inferred from NEAs taxonomic classification. However, one of the results of this study, Chapter 5, is the identification of a trend of the dependence of the NEATM best-fit parameter η with the phase angle. The best linear fit to the observed distribution of NEAs η-values is: $\eta=(0.011\pm0.002)\alpha+(0.90\pm0.07)$, where α is the phase angle. This linear dependence can be used as the best estimate for the default η-value. However, given the accuracy of the fit, diameters and albedos in significant agreement are obtained if default η-values of 1.0 for $\alpha<45^\circ$ and of 1.5 for $\alpha\geq45^\circ$ where α indicates, as usual, the phase angle.

4.2.1 Diameters, albedos and η-values derived from observations at Keck

Object	D_{eff} (km)				p_v			Tax Class	Notes
	STM	NEATM	η	FRM	STM	NEATM	FRM		
1627 Ivar	7.94	**9.12**	(1.0)	15.9	0.20	**0.15**	0.050	S	Lc corrected
1866 Sisyphus	7.47	**8.48**	(1.0)	16.3	0.20	**0.15**	0.042	S	Lc amp. small
2100 Ra-Shalom	1.60	**2.79**	2.32	2.60	0.25	**0.083**	0.095	Xc	Lc corrected
4034 1986 PA	0.40	**0.42**	(1.0)	0.57	0.58	**0.52**	0.29	O	
4055 Magellan	2.20	**2.49**	(1.0)	4.36	0.39	**0.31**	0.10	V	
4660 Nereus	0.26	**0.33**	(1.5)	0.33	0.86	**0.55**	0.54	Xe→E	
5587 1990 SB	3.56	**3.57**	0.84	5.14	0.51	**0.50**	0.24	Sq	Lc corrected
5604 1992 FE	0.52	**0.55**	(1.0)	0.77	0.69	**0.61**	0.32	V	
5751 Zao	1.80	**2.30**	(1.5)	2.53	0.58	**0.36**	0.29	X →E	Lc amp. small
14402 1991 DB	0.56	**0.60**	1.04	0.81	0.17	**0.14**	0.08	C	Lc amp. small
15817 Lucianotesi	0.30	**0.32**	(1.0)	0.47	0.73	**0.64**	0.29	X→E	
16834 1997 WU_{22}	1.51	**2.00**	(1.5)	2.06	0.53	**0.30**	0.29	S	
19356 1997 GH_3	0.83	**0.91**	0.98	1.45	0.41	**0.34**	0.13	S	
25330 1999 KV_4	2.34	**3.21**	1.50	3.41	0.098	**0.052**	0.046	B	Lc amp. small
1999 FK_{21}	0.58	**0.59**	0.91	0.85	0.33	**0.32**	0.15	S	
1999 NC_{43}	1.22	**2.22**	2.86	1.62	0.47	**0.14**	0.27	Q	Lc corrected
2000 BG_{19}	1.88	**1.77**	0.74	3.25	0.038	**0.043**	0.013	X →P	
2000 PG_3	3.90	**4.60**	(1.0)	8.59	0.059	**0.042**	0.012	D	Lc amp. small
2000 EV_{70}	0.14	**0.15**	(1.0)	0.22	0.68	**0.60**	0.29	Q	
2001 FY	0.30	**0.32**	(1.0)	0.48	0.59	**0.52**	0.23	S	
2001 HW_{15}	0.16	**0.18**	(1.0)	0.27	0.54	**0.43**	0.20	?	
2002 BM_{26}	0.41	**0.84**	3.10	0.57	0.094	**0.023**	0.050	X →P	
2002 CT_{46}	0.15	**0.16**	(1.0)	0.24	0.36	**0.32**	0.15	Sr	

Table 4-1 Diameters and albedos from thermal model fits to infrared observations obtained at Keck. NEATM's diameters and albedos are given in boldface. On the basis of results of this work, Chapter 5 and Chapter 6, we take those values as our best estimate for NEAs diameters and albedos. The estimated overall uncertainties in the NEATM values of diameter and albedo are 10 and 20%, respectively for observations carried out at phase angles smallter than 40°. At larger phase angles such error increase for increasing η-values. For $1<\eta<1.5$ NEATM albedo uncertainty is about 40%. For phase angles larger than 40° and η-values larger than 1.5 NEATM albedos are likely to be underestimated by about 35% and they uncertanites of about 40% (see Chapter 6). D_{eff} is the diameter of a sphere presenting the same projected area to the observer. Values of η in brackets are phase-angle dependent default values chosen onthe basis of the results of this study. Taxonomic classes are from Bus and Binzel (2002), Binzel et al. (2002) and the results of Binzel et al. (2004), with the exceptions of (4055) Magellan (Cruikshank et al., 1991).

For convenience diameters, albedos and η-values derived from observations obtained at Keck are reported here in Table 4-1. Note that Table 4-1 contains derived physical parameters for three more objects, 15817 Lucianotesi, 2000 EV_{70} and 2001 HW_{15}, which were not included in Delbò et al., (2003) work. Their detection in LWS co-added frames was made possible by an accurate method of registering nod-sets – described in section 3.7 – developed in this work. Table 4-2 lists novel results obtained from ESO observations, whereas Table 4-3 shows diameters, albedos and η-values obtained from the radiometric observations carried out at the NASA-IRTF.

4.2.2 Diameters, albedos and η-values derived from observations at ESO

Object	D_{eff} (km)				p_v			Tax Class	Notes
	STM	NEATM	η	FRM	STM	NEATM	FRM		
5381 Sekhmet	1.05	**1.3**	(1.5)	1.5	0.4	**0.25**	0.2	S	
		1.5	1.9			**0.22**			
5587(1990 SB)[15]	3.4	**4.0**	1.1	6.7	0.35	**0.25**	0.09	Sq	LC corr N-Spec
	3.5	**3.74**	(1.0)	5.78	0.34	**0.29**	0.12		LC corr N-Filters
5604(1992 FE)	0.7	**0.7**	(1.0)	1.1	0.3	**0.3**	0.12	V	$p_V$error~40%
12008	3.55	**3.76**	(1.0)	5.35	0.81	**0.72**	0.36	-	
19356(1997GH_3)	0.95	**1.0**	(1.0)	1.4	0.3	**0.29**	0.14	S	Large scatter
25143 Itokawa	0.20	**0.37**	(1.5)	0.22	0.61	**0.19**	0.54	S	ESO08apr01
		0.33	1.2			**0.23**			
33342(1998 WT_{24})	0.28	**0.37**	(1.5)	0.38	0.84	**0.50**	0.48	E	Dec 04, 2001
35396(1997 XF_{11})	0.75	0.80	(1.0)	1.16	0.45	0.40	0.19	Xk→E	H: this work
		0.89	1.3			**0.32**			LC corr.
25330 (1999 KV_4)	2.26	**2.5**	(1.0)	4.16	0.1	**0.09**	0.03	B	LC ampl. small
		2.7	1.2			**0.08**			
2001 LF $_{(3Jun03)}$	1.5	**2.0**	1.4	2.5	0.08	**0.05**	0.03	C	N + Q Jun,3
		2.1	(1.5)			**0.04**			
2001 LF $_{(2Jun03)}$	1.7	**1.9**	(1.5)	2.2	0.1	**0.06**	0.04	C	N band only
		1.67	1.1			0.07			
2001QP	3.7	**4.0**	(1.0)	6.0	0.22	**0.19**	0.08	-	
2002 AV_4	1.1	**1.5**	(1.5)	1.4	0.73	**0.38**	0.43	-	
		1.54	1.57			**0.37**			
2002 QE_{15}	1.15	**1.49**	(1.5)	1.63	0.40	**0.24**	0.20	-	

Table 4-2 Diameters and Albedos from Thermal Model Fits of ESO targets. See Table 4-1 caption for further details. Taxonomic classes are from Bus and Binzel (2002), Binzel et al. (2002) and the results of Binzel et al. (2004) with the exception of 2001 LF which is from Dandy et al., 2003; 1998 WT24 which is from Kiselev et al., (2002) and 5381 Sekmeth which is from Nolan et al., (2003)

[15] Mean of the two N-band spectra.

It is worth to stress again that our data set contains asteroids which have been observed with different instruments and under different observing geometries.

Comments on the derivation of albedo and diameters for each individual object are given in section 4.3. Extensive comments on the target observed at Keck are given in Delbò et al., (2003).

4.2.3 Diameters, albedos and η-values derived from observations made at the NASA-IRTF

Object	D_{eff} (km)				p_v			Tax Class	Notes
	STM	NEATM	η	FRM	STM	NEATM	FRM		
1580 Betulia	3.54	**4.35**	1.27	5.06	0.17	**0.11**	0.08	C	
6489 Golevka	0.30	**0.33**	(1.0)	0.47	0.46	**0.39**	0.18	Q	
5381 Sekmeth	-	1.3	1.5	-	-	0.25	-	S	α=25
5381 Sekmeth	1.0	1.4	1.7	1.62	0.42	0.24	0.17	S	α=29
5381 Sekmeth	-	1.2	1.3	-	-	0.3	-	S	α=33
5381 Sekmeth	1.0	1.4	1.8	1.55	0.45	0.24	0.18	S	α=38
5381 Sekmeth	-	1.4	1.9	-	-	0.22	-	S	α=42
25330 1999 KV_4		2.55	1.06			0.084		B	
35396 (1997 XF_{11})	0.81	**0.91**	1.2	1.07	0.39	**0.31**	0.22	Xk→E	*05nov02* H from ESO
	0.83	**1.18**	1.8	1.05	0.37	**0.18**	0.23	Xk→E	*03nov02* H from ESO
33342(1998 WT_{24})	0.32	**0.34**	0.9	0.40	0.68	**0.59**	0.43	E	18dec01 no LCC
	0.32	**0.44**	1.5	0.38	0.66	**0.35**	0.48	E	19dec01 no LCC
	0.31	**0.50**	1.85	0.36	0.70	**0.27**	0.53	E	21dec01 no LCC

Table 4-3 Diameters and Albedos from Thermal Model Fits of IRTF targets. See Table 4-1 caption for further details. Taxonomic classes are from Bus and Binzel (2002), Binzel et al. (2002) and the results of Binzel et al. (2004) with the exception of 2001 LF which is from Dandy et al., 2003; 1998 WT24 which is from Kiselev et al., (2002) and 5381 Sekmeth which is from Nolan et al., (2003)

4.3 Comments on individual asteroids

The results listed in Table 4-1, Table 4-2 and Table 4-3 should be analized by taking into account the following notes on individual objects. We note that for several objects, the measured albedo is a decisive parameter for determining a unique taxonomic class. In the taxonomic system of Tholen (1984) and Bus (1999), objects having neutral spectra within the X-complex typically display three categories of albedos. The "X" designation for an object is resolved into the classes E, M, or P based on its having a high, moderate, or low albedo, respectively. For the objects originally tabulated by Bus and Binzel (2002) or Binzel et al. (in preparation) as belonging to the X-complex, we indicate our resolution of the spectral degeneracy from X to (→) E, M, or P.

4.3.1 15817 Lucianotesi (1994 QC)

No lightcurve data are available for the time of the Keck observations. The scatter of the flux values does not allow η to be adequately constrained; therefore the results given in Table 4-1 for the NEATM were obtained assuming a default value for η of 1.0 (see Fig. 4.1).

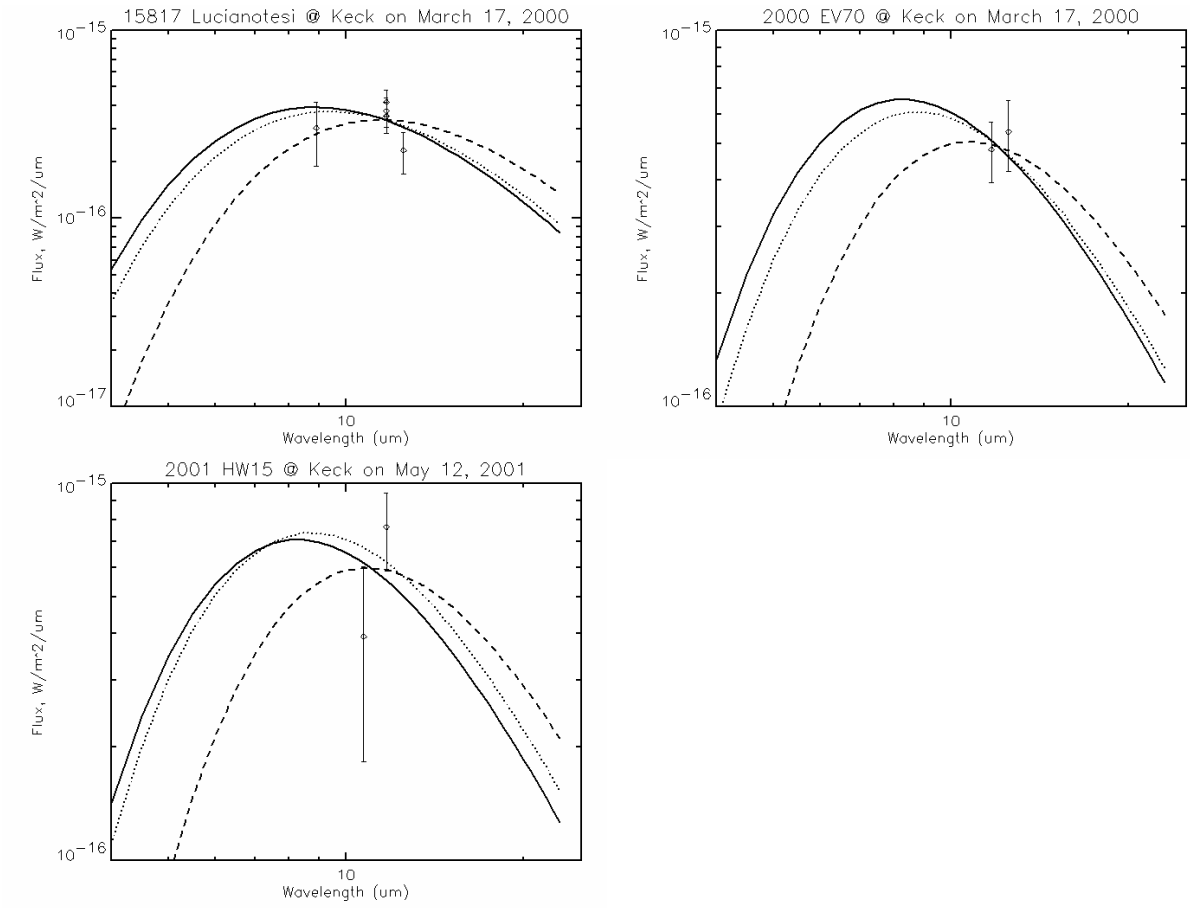

Fig. 4.1 Thermal model fits to observed infrared fluxes for 15817 Lucianotesi, 2000 EV_{70} and 2001 HW_{15} obtained at Keck and not included in Delbò et al. (2003) work. Continuous line: STM, dashed line: FRM; dotted line: NEATM with default η-value of 1.0

The results indicate a very high albedo (though its uncertainty from photometry is of ~ 0.1), which is consistent with refining the taxonomic type from X- to E-type. The identification of E type asteroids is important for our understating of dynamical transport mechanisms from the source region to the near-Earth space. E-type are, for instance, abundant amongst Hungaria asteroids.

4.3.2 2000 EV_{70}

Thermal infrared data, obtained in two filters only, do not allow η to be constrained adequately (see Fig. 4.1). I have resorted to the default value for η of 1.0 for the NEATM. The derived albedo is very high and it makes 2000 EV_{70} the smallest object for which radiometric diameter has been measured. Note that the albedo uncertainty is very large, 0.13, given the low signal to noise ratio of the thermal infrared photometry. Moreover, no lightcurve data are available for the time of the Keck observations which makes the uncertainty of the radiometric results even larger.

4.3.3 2001 HW_{15}

The source was extremely weak in the 11.7 and in the 10.7 μm filters. The latter measurement is affected by a large uncertainty: about 50%. The resulting error on the albedo is therefore of the order of 0.2 (see Fig. 4.1). No lightcurve data are available and no estimation for the lightcurve amplitude, rotational period and taxonomic class are at present at disposal.

4.3.4 25143 Itokawa (formerly known as 1998 SF_{36})

25143, recently named **Itokawa,** is the target of the successfully launched Japanese sample-return mission Hayabusa (Muses-C), which will rendezvous with this target in June 2005. V band CCD data were obtained simultaneously to the thermal infrared observations using the DFOSC installed at the 1.5m Danish telescope. Observations were carried out on April 8, 2001 between 09:27 UT and 10:14 UT and on April 9, 2001 between 09:17 and 10:14 UT. However, this two time intervals were long enough only to cover a small fraction of the asteroid lightcurve period. Nevertheless, using a simplified tri-axial ellipsoid model[16] with the rotational period, pole and shape solution of Kaasalinen et al. (2003), I have generated a synthetic lightcurve which was fitted to the data. The best fit (see Fig. 4.2) was obtained with an absolute rotational phase φ_0 = -32.5° at JD=2452007.5.

On the basis of the synthetic lightcurve, note that thermal infrared observations were carried out near lightcurve maximum. Differential correction factors for each infrared observation were calculated, but the largest of these was found to be of 0.11 magnitudes i.e. less then 10% in flux. The synthetic lightcurve, based on the simple variation of the illuminated area projected along the observer direction, shows amplitude of 1.77 magnitudes. The aspect angle at the time of lightcurve maximum was 71.5° and

[16] See A. Pospieszalska-Surdej & Surdej (1985) for details.

the sub-Earth longitude ψ=320º. The aspect angle with respect to the Sun was 95.5º, the object was therefore almost equator on if seen from the Sun. The asteroid rotational phase with respect to the Sun ψ_{Sun} was equal to 24º at the time of lightcurve maximum which occurred at 10.3 UT on April 09, 2001. The H magnitude to be used as input parameter for the thermal model has to be corrected to take into account the geometry at the time of the thermal observation. Abe et al. (2002), derived H = 19.9 0±0.10 calculating the mean magnitude at 90 degrees of aspect angle.

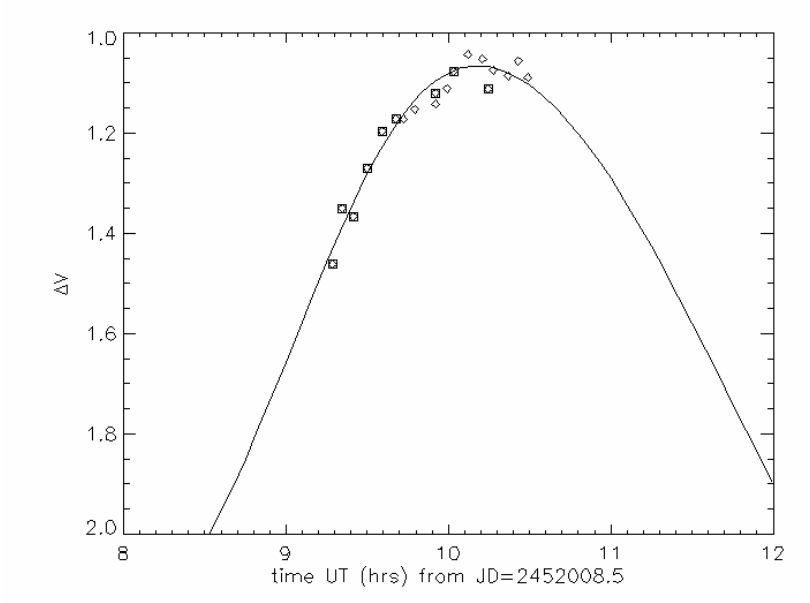

Fig. 4.2 Synthetic lightcurve of the asteroid 1998 SF36 and the best fit to the observed V-band data. Measurements obtained on 9 April, 2001 have got a square symbol superimposed. The two lightcurves were composited on the 12.13 hours sidereal period basis.

The illuminated portion of a triaxial ellipsoid can be easily obtained using the following expression adapted from A. Pospieszalska-Surdej & Surdej (1985):

$$S = \pi abc\sqrt{\sin^2 A_{Sun}\left(\frac{\sin^2\psi_{Sun}}{a^2}+\frac{\cos^2\psi_{Sun}}{b^2}\right)+\frac{\cos^2 A_{Sun}}{c^2}} \qquad (4\text{-}1)$$

and the mean magnitude at $A_{Sun} = 90^o$ by taking -2.5 times the logarithm of $\langle S \rangle$ i.e.

$$\langle S \rangle = \frac{1}{\pi}\int_0^{\pi} S(\psi_{Sun}, A = 90^o)\, d\psi_{Sun} = \pi abc\sqrt{\sin^2 A_{Sun}\left(\frac{1}{2a^2}+\frac{1}{2b^2}\right)+\frac{\cos^2 A_{Sun}}{c^2}} \qquad (4\text{-}2)$$

The correction to the H value is simply equal to -2.5log(S/$\langle S \rangle$). Inserting the numerical values into Eq. (4-2) and Eq. (4-1) I have derived the actual absolute magnitude H_{actual} at the time of thermal IR observations to be H=19.7.

The STM the FRM and the NEATM were fitted to the thermal IR data (see Fig. 4.3). The derived effective diameters and geometric albedos are reported in Table 4-2. Note the agreement of the NEATM's results with the published diameter and albedo by Sekiguchi et al. (2003). The NEATM best fit were obtained with $\eta = 1.2 \pm 1.0$, which is reasonably below the value suggested by Delbo et al. (2003) to be displayed by NEAs at such large phase angle. However, the fitted η value is not very well constrained: fluxes were obtained for a limited number of wavelengths in the N band (the object was not bright enough for fluxes in the 5 and 20 μm ranges to be obtained) and their errors of about 10%. The large error on the fitted η and therefore on our estimate of the actual color temperature makes the size and albedo determination not very reliable: $\sigma_D \approx 35\%$ and $\sigma_{Pv} \approx 50\%$. A more stable solution ($\sigma_D \approx 3\%$ and $\sigma_{Pv} \approx 5\%$.) can be found by fixing the η value to 1.5 on the basis of the Delbo et al. (2003) results.

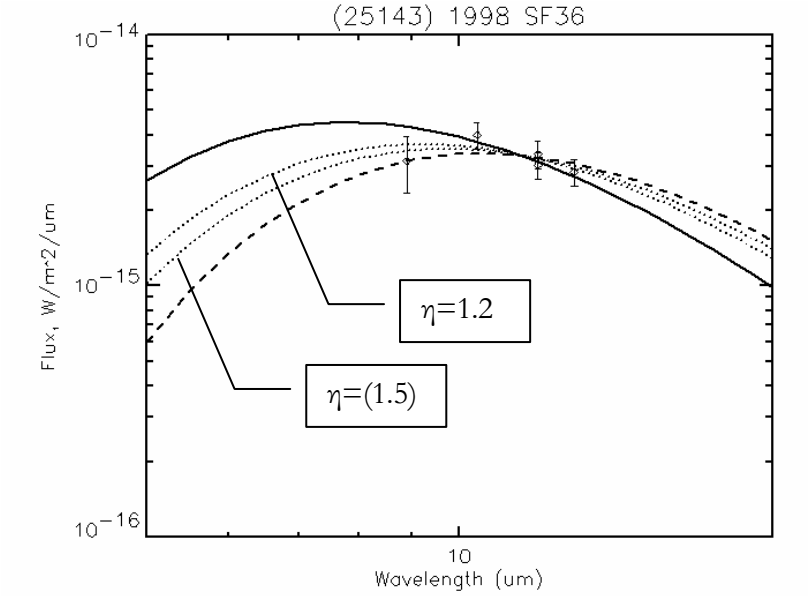

Fig. 4.3 Thermal models fit to the observed infrared flux for 25143 Itokawa. Continuous line: STM, dashed line: FRM; dotted line: NEATM with default η-value of 1.2 and 1.5

Thermal IR data obtained on April 09, 2001 are of poorer quality and have not been included in this analysis so far.

4.3.5 2001 LF

N and Q band data were obtained on June 03, 2004 at the 3.6 m telescope at ESO. P. Pravec and colleagues (Pravec, personal communication) got lightcurve data for this object from late June/early July 2003 from the Ondrejov observatory and the observatory of the University of Western Ontario. Although the solution is uncertain, 2001 LF appears to have a rotational period of about 10 hours with a lightcurve amplitude within 0.2 magnitudes. The object is classified as a C-type by Dandy et al (2003). The H value used as input parameter for thermal models has been obtained from Dandy's et al. work. The G value was assumed to be equal to 0.15 given the taxonomic type of this asteroid as suggested by Bowell et al. (1989). Given the not dramatically large lightcurve amplitude, no lightcurve correction was applied to the thermal infrared flux. Fig. 4.4 shows STM, FRM and NEATM fits to data points. NEATM gives a stable solution (i.e. $\sigma_D \approx 4\%$, $\sigma_{Pv} \approx 5\%$, $\sigma_\eta = 7\%$). The derived η-value of 1.4 ± 0.1 is in good agreement with the value expected on the basis of Delbo et al. (2003) results. The NEATM derived albedo of 0.05 is consistent with the C-type classification for this asteroid.

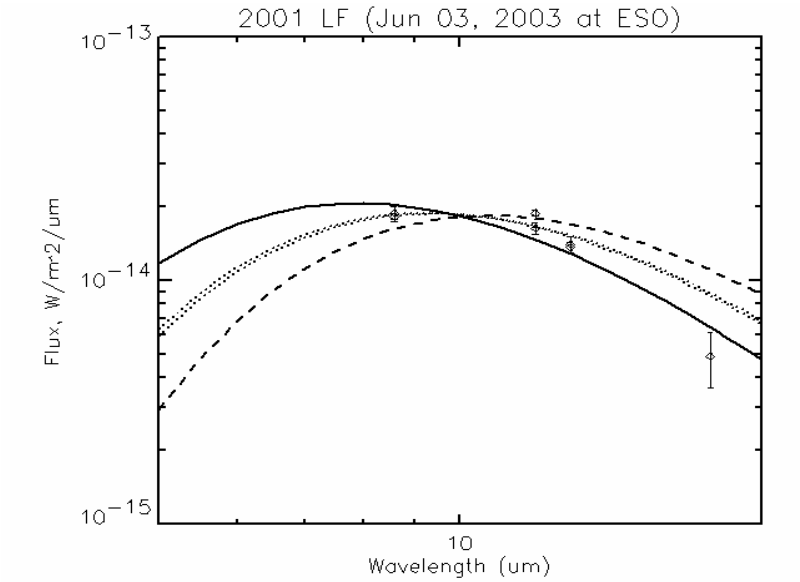

Fig. 4.4 Thermal models fit to the 2001 LF data observed on June 03, 2003. No correction for lightcurve was applied. Continuous line: STM, dashed line: FRM; dotted lines: NEATM Note how, in this case, the fitted η-value is very close to its default value of 1.5

Apparently, the flux measured at 17.8 μm (Q1 filter) is lower than what expected from thermal models fits (see Fig. 4.4). The presence of thin cirrus, noted at down, might have affected the reliability of the absolute photometry especially in the Q band. Furthermore, the method used to obtain the Q-band measurement was subject to possible loss of flux. A slowly drift of the asteroid in the TIMMI2

field of view due small tracking errors of the telescope was noted while images in the N-band filters were acquired. The integration in the Q1 filter was almost one hour long and divided into 8 nodsets. Shifting each nod-set before co-adding was thus necessary to avoid smearing effects and compromise the detection of the object. Unfortunately, the source was not visible on each nod-set. To properly register the nod-sets and, the exposures in the Q1-filter were bracketed by two 11.9μm-images, where the asteroid was clearly visible (see Fig. 4.5).

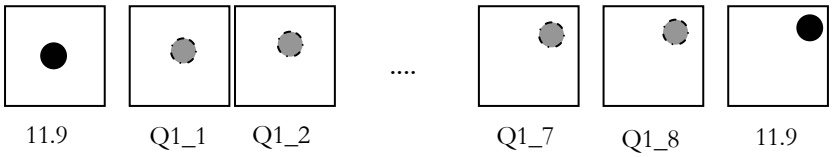

Fig. 4.5 Observing sequence used to image 2001 LF in the Q-band at the 3.6 m telescope with TIMMI2. Q1_1 represent the first nod-set Q1_8 the eighth. The gray round patch indicates the position of the source moving on the detector array and below detection on each exposure. The black circle corresponds to the position of the object on 11.9μm-images where the asteroid was detected.

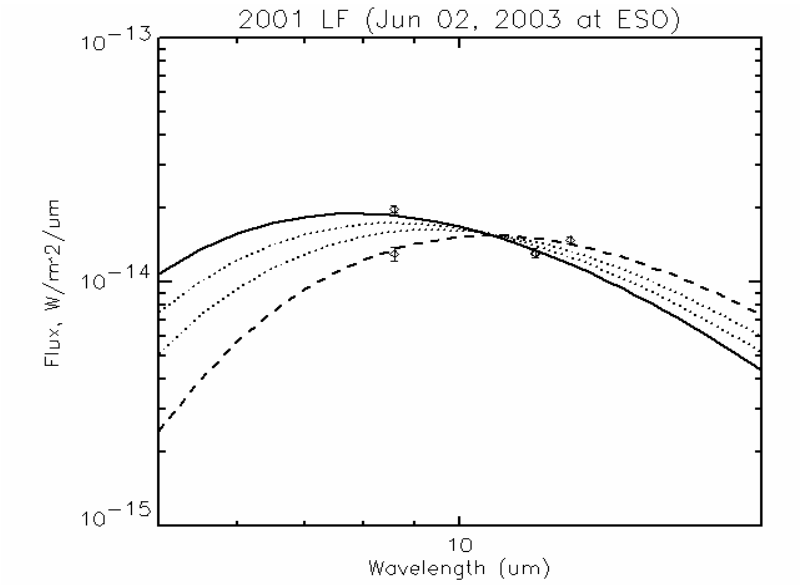

Fig. 4.6 Thermal models fit to the 2001 LF data observed on June 02, 2003. Continuous line: STM, dashed line: FRM; dotted lines: NEATM In this case, the fitted η-value of 1.1 is lower than its default value of 1.5

On the basis of the position of the asteroid on the two 11.9μm-exposures, its drift motion as a function of time was calculated and the differential shifts for each nod-set calculated. Finally, Q1-nod-sets were co-added taking into account of the appropriate shifts.

Data of 2001 LF, although of lower quality, were obtained on June 02, 2003 as well. A large variation in the flux at 8.6 μm is visible, though at 11.9 μm such variation in the flux is not visible. Even though just N band flux were measured, the NEATM η value is well constrained to 1.1 ± 0.1. The resulting diameter of 1.67 km is a lower than the value obtained by using the default $\eta=1.5$, but given the uncertainties, the agreement is good.

4.3.6 5381 Sekmeth

This asteroid was found to be a binary system in radar images (Nolan et al., 2003) with a rotation period of the primary of about 3 hours (P. Pravec, 2003) and the orbit of the secondary not well constrained, but probably of the order of a day. V band CCD data, along with thermal infrared observations, were obtained on June 02, 2003. Unfortunately, the non photometric quality of the night did not allow an absolute calibration of the V magnitude of the asteroid to be performed. However, the differential photometry indicates a lightcurve amplitude of about 0.35 mag. A fit of a synthetic lightcurve to the uneven and sparse data sample are in favor of a rotational period longer than 3 hours: we have obtained a good visually solution with a sidereal rotational period of about 3.6 hours (see Fig. 4.7). Correction factors for each thermal infrared observation have been calculated on the basis of the synthetic lightcurve, which assumes the variation in brightness of the asteroid to be proportional to the illuminated projected area seen by the observer. As discussed by Delbò et al. (2003) the assumption of the thermal lightcurve to have the same amplitude and phase of the one observed in reflected light might cause errors in the final diameters and albedos difficult to be estimated. Nevertheless, results of the thermal modeling using both the lightcurve-corrected and uncorrected data are in good agreement and they indicate the color temperature of the asteroid to be lower than the STM prediction: although only N band data have been obtained, the STM fit to the thermal continuum is poor (see Fig. 4.8 (a) and (b)).

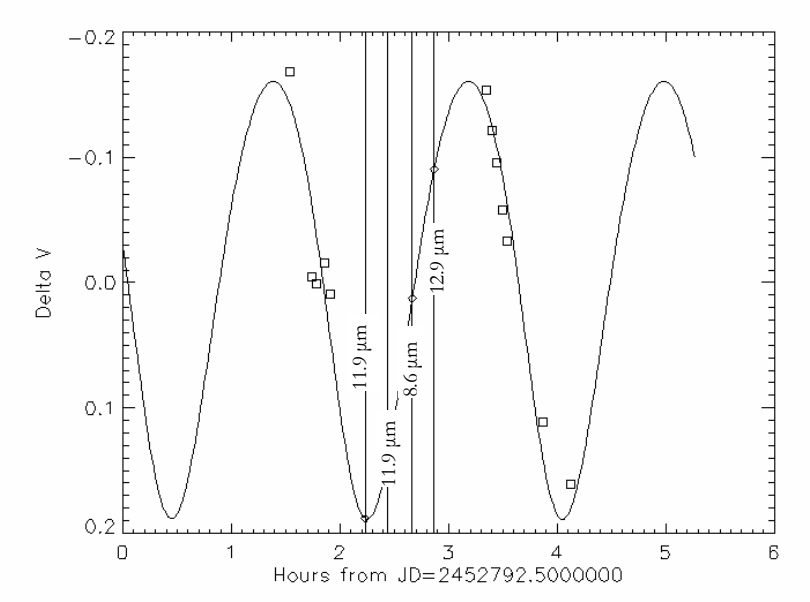

Fig. 4.7 The synthetic light curve (continuous line) fitted to the differential V magnitudes (squares) obtained on June 02, 2003 with WFI at 2.2m ESO/MPI telescope. Vertical lines are drawn in correspondence with the epoch of thermal infrared observations.

Given the uncertainties of the fluxes and the non photometric quality of the night (deduced from the analysis of the visible CCD frames) η is not well constraind. I have therefore carried out a study of the NEATM derived diameter and albedo as a function of the input value for η. Results for both lightcurve corrected and lightcurve uncorrected data are shown in Fig. 4.8

Lightcurve corrected		Raw (no lightcurve correction)		
D(km)	Pv	D (km)	Pv	η
1.03	0.42	1	0.44	0.756
1.15	0.34	1.12	0.35	1
1.27	0.28	1.24	0.29	1.25
1.51	0.2	1.47	0.21	1.8
		1.65±0.43	0.16±0.09	2.3±1.2
1.51±0.37	0.22±0.10			1.9±0.9
1.08	0.38	1.06	0.4	0.756 (STM)
1.55	0.18	1.51	0.19	- (FRM)

Table 4-4 Derived diameters and albedos by means of the NEATM as a function of the η-value. If η is derived by fitting the observed spectral energy distribution, error estimates are reported.

Judging from the fit to the thermal infrared continuum, the best solution appears to indicate an effective diameter between 1.3 and 1.5 km and an albedo between 0.28 and 0.22 for 5381 Sekmeth. The

color temperature of the object seems to be lower than that suggested by Delbò et al (2003) for the behavior of common NEAs: i.e. η=1.25 produces a poorer fit to the thermal infrared continuum. 5381 Sekhmet, like some other binaries, has rather high η. Interestingly, results from IRTF observations (Mueller et al, 2003) indicate D=1.38 and Pv=0.24 in perfect agreement with this the ESO data set. Such results are included in this work.

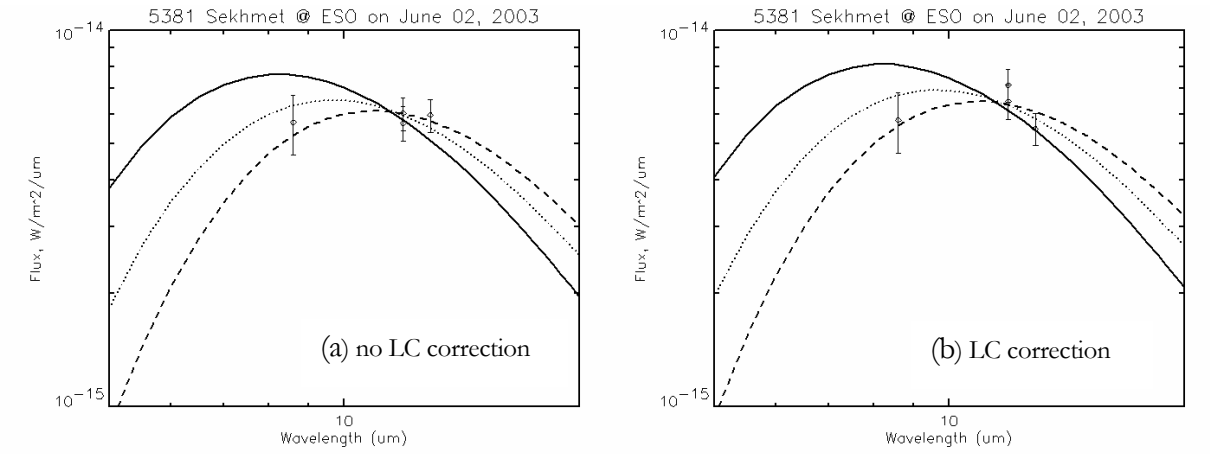

Fig. 4.8 Thermal models fit to the 5381 Sekhmet data observed on June 02, 2003. No correction for the lightcurve has been performed in plot (a), whereas data points in plot (b) have been corrected for lightcurve.

However, the radar effective diameter $D_{radar} = 2\sqrt{R_{Max}^2 + R_{Min}^2}$ calculated on the basis of the size of the primary, $R_{Max} = 0.5km$, and that of the companion, $R_{Min} = 0.15km$, is close to 1km (Nolan et al., 2003). Given the H-value of 16.5, the resulting albedo of 0.40 is higher than what expected from the S-type classification of this object. In this respect, our radiometric albedo is consistent with the stony composition inferred from spectroscopic observation carried out at Kitt Peak (Nolan et al., 2003).

4.3.7 25330 (1999 KV$_4$)

V band CCD data obtained with WFI at the 2.2m ESO/MPI telescope suggests a lightcurve amplitude of about 0.1 magnitudes, in agreement with Delbò et al. (2003) and with the summary of "pre-published" periods of NEAs of Pravec et al. (http://sunkl.asu.cas.cz/~ppravec/newres.htm). Given that small lightcurve amplitude (about 10% in flux), no correction were applied to the thermal infrared fluxes. The NEATM yields the best fit to the data points as shown in Fig. 4.9. The derived albedo of 0.08±0.02 is higher than the value obtained from the observations carried out at Keck (i.e.

0.052), thought still compatible with the B taxonomic classification of this object. STM and FRM produce poorer fits, as visible in Fig. 4.9. NEATM predictions, obtained both by fitting η (which resulted equal to 1.2±0.3) and fixing its value to 1.0 (according to Delbo et al., 2003 for observations made at phase angle less than 45°) are shown in Fig. 4.9 with dotted lines. Derived diameter and albedo are listed in Table 4-2.

NEATM fit to MIRLIN observations carried out at the NASA-IRTF at the very small phase angle of 3° yields a diameter of 2.5 km and an albedo of 0.08 in perfect agreement with the ESO data set (see Mueller et al., 2003).

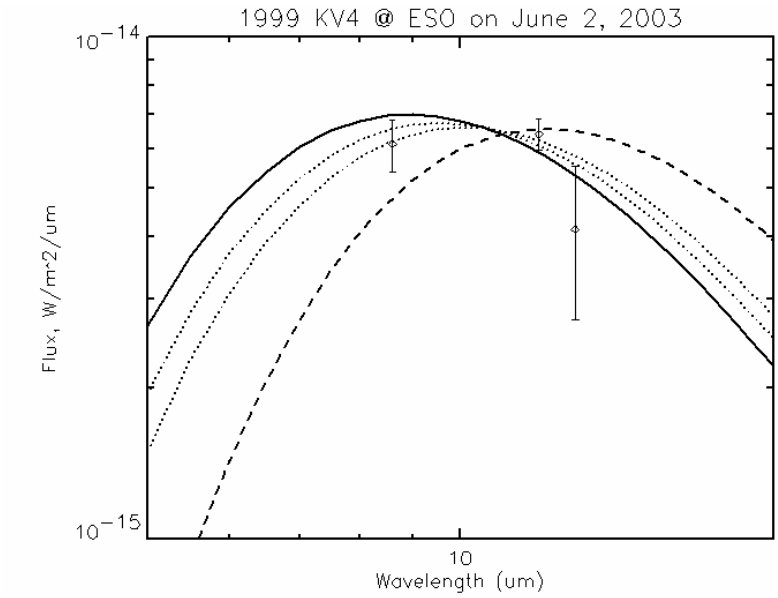

Fig. 4.9 Thermal model fits to multi-filter photometry of the NEA 1999 KV_4 obtained at the ESO 3.6m telescope. Continuous line: STM, dashed line: FRM; dotted line: NEATM with η=1.0 (the one closer to STM prediction) and with η=1.2.

4.3.8 2002 AV_4

This asteroid has been classified with an Apollo-type orbit. A preliminary solution to the V-band CCD data indicates a lightcurve amplitude of about 0.3 magnitudes and most likely a rotational period of 2.9 hours. Neither the FRM nor the STM are able to provide a good fit to the thermal infrared continuum. NEATM best fits with η=1.57±0.25 (Fig. 4.10). Resulting diameter and albedo are listed in Table 4-2.

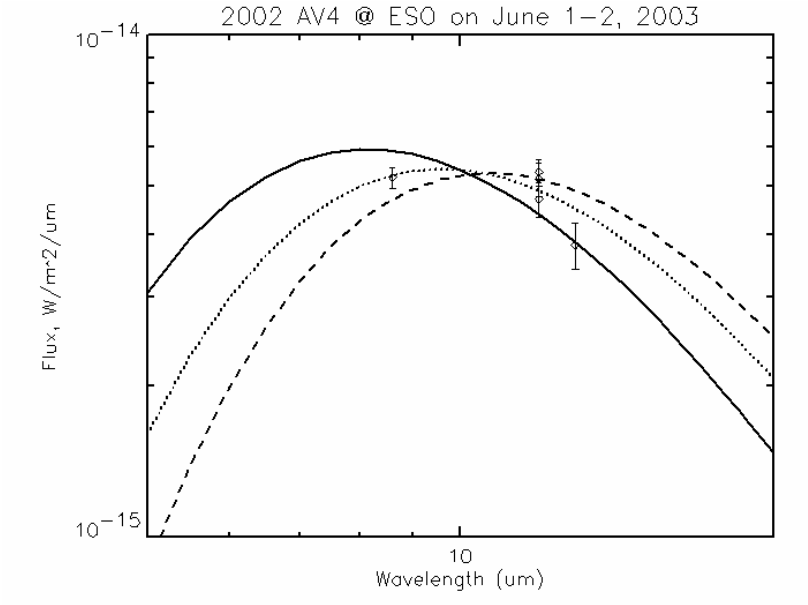

Fig. 4.10 Thermal model fits to multi-filter photometry of the NEA 2002 AV_4 obtained at the ESO 3.6m telescope. Continuous line: STM, dashed line: FRM; dotted line: NEATM.

4.3.9 5587 (1990 SB)

Lightcurve data are derived from photometry obtained during the April 2001 apparition by Pravec and colleagues (Pravec personal communication, 2000). Visible CCD observations obtained with the DFOSC at 1.5m Danish telescope covering a bit more than one hour were also obtained. The Pravec et al. and the ESO lightcurve superimpose nicely (both data set are not absolute calibrated: this superposition was achieved by arbitrarily sliding the lightcurves vertically). The synthetic lightcurve has been generated assuming the asteroid to have a tri-axial ellipsoidal shape and geometric scattering to be valid. The fit of the synthetic lightcurve to the observed ones has been obtained by varying the ratio of the semisaxis a/b parameter and the absolute rotational phase of the asteroid. The differential correction factors to the thermal infrared fluxes were calculated with respect to the mean magnitude of the visible lightcurve. Fig. 4.11 shows the three lightcurves.

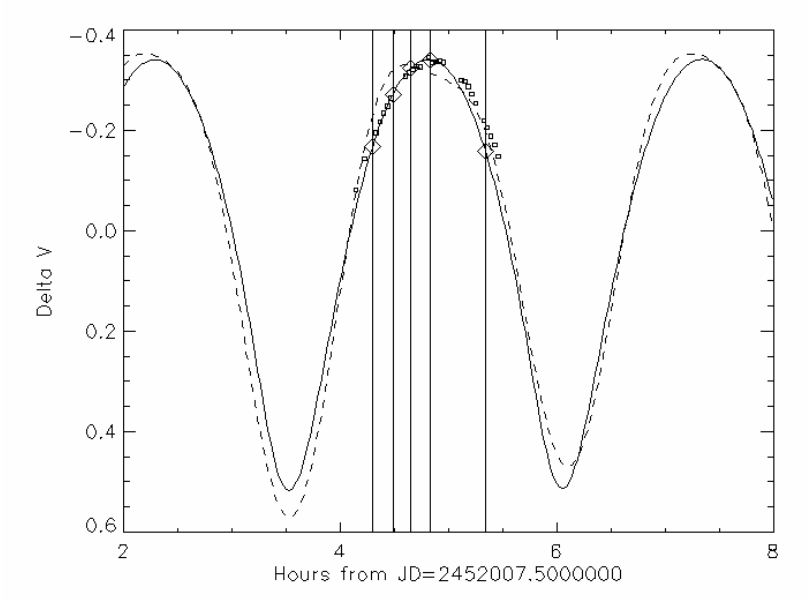

Fig. 4.11 Continuous line represent the synthetic lightcurve generated assuming the asteroid to be a triaxial ellipsoid with a geometric scattering law. Dashed line is the Pravec el al. lightcurve. Small squares are the DFOSC observations. Vertical lines are drawn in correspondence to the thermal infrared observations. Differential correction factors are of less than 0.2 magnitudes.

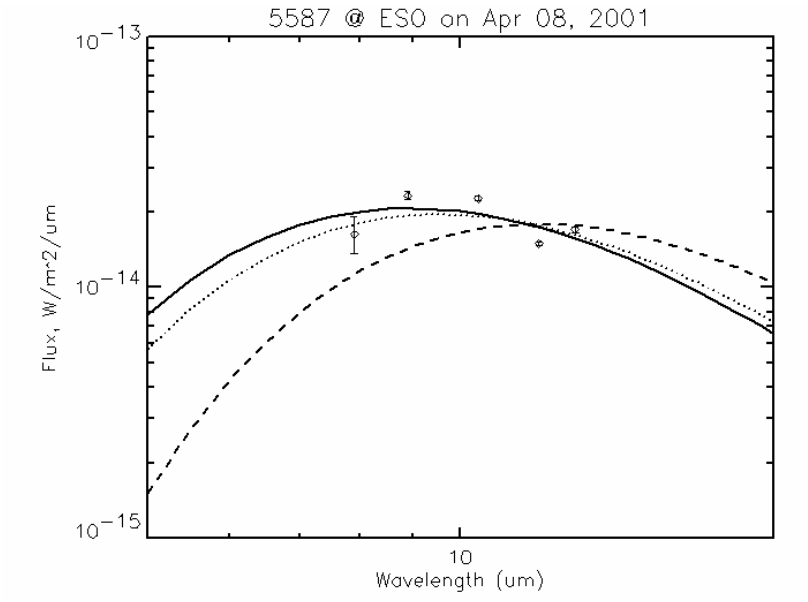

Fig. 4.12 Thermal infrared photometry of the NEA 5587 obtained at ESO and thermal models fits. Continuous line: STM, dashed line: FRM; dotted line: NEATM.

Photometric observations at 7.9, 8.9, 10.4, 11.9 and 12.9 μm were carried out on April 08, 2001. The diameters and albedos derived by fitting thermal models to the lightcurve corrected infrared fluxes are

reported in Table 4-2. Note the good agreement of NEATM solution with the Delbo et al., (2003) results. These photometric data indicate a relatively high color temperature for the surface of this NEA. The STM produce a good fit as well and its results are in agreement with the NEATM ones, given the uncertainties.

Furthermore, given the infrared brightness of this target, N- and Q-band spectra were successfully obtained on the following night. The correction for the lightcurve does not modify the shape of the thermal infrared continuum, since fluxes at different wavelengths were all measured simultaneously. However, the H value must be varied according to the (mean) projected area the asteroid showed to the Sun during the time of the spectroscopic observations. The reference epoch for the spectroscopic observation was taken at that time when half of the integration was completed.

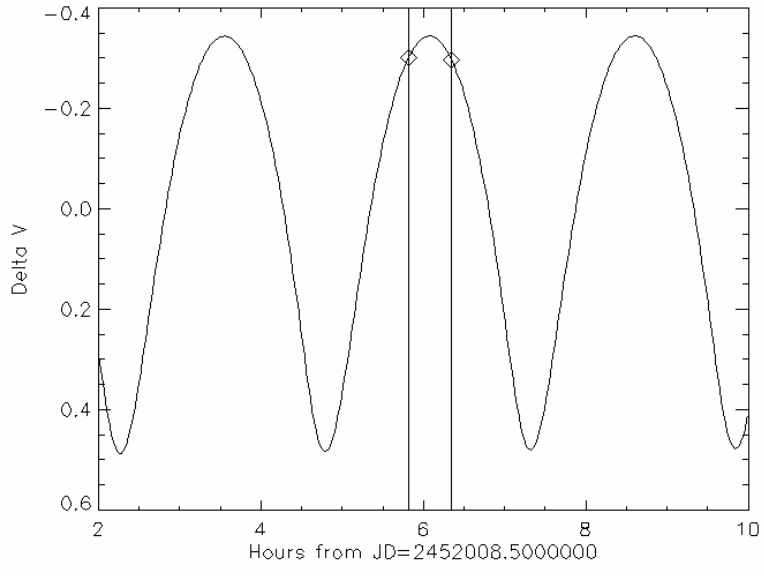

Fig. 4.13 The continuous sinusoidal line represents the visible lightcurve as in the case of Fig. 4.11.Vertical lines are drawn in correspondence with the epochs of the thermal spectroscopy measurements.

The NEATM derived a diameter of 4.1±0.3 km and an albedo of 0.25±0.03 from the first spectrum. The determination of the color temperature was reliable η=1.0±0.1 and in agreement with Delbo et al., (2003) predictions. The STM fits with a lower diameter equals to 3.8 km and a higher albedo of 0.28. The FRM, which does not provide a reliable fit to the thermal continuum, gives a diameter of almost 7 km and a very low albedo of 0.08 inconsistent with the S class taxonomic classification of this object. If lightcurve correction is not taken into account, NEATM fits with a diameter 12% higher and an albedo

32% lower. η is conserved, since the lightcurve correction do not alter the shape of the thermal continuum but it does shift only its overall level.

NEATM fits the second spectrum with a diameter of 4.0±0.3km, an albedo of 0.25±0.03 and η=1.0±0.1. The STM and the FRM give results within 3-5% of those obtained by fitting the first spectrum. Given the uncertainties, the radiometric results derived from the two spectroscopic observations and from the filter photometry are in good agreement.

The diameter derived from ESO observations is about 10% larger than the value derived from radiometry made at Keck. The resulting albedo is thus smaller of about 20%.

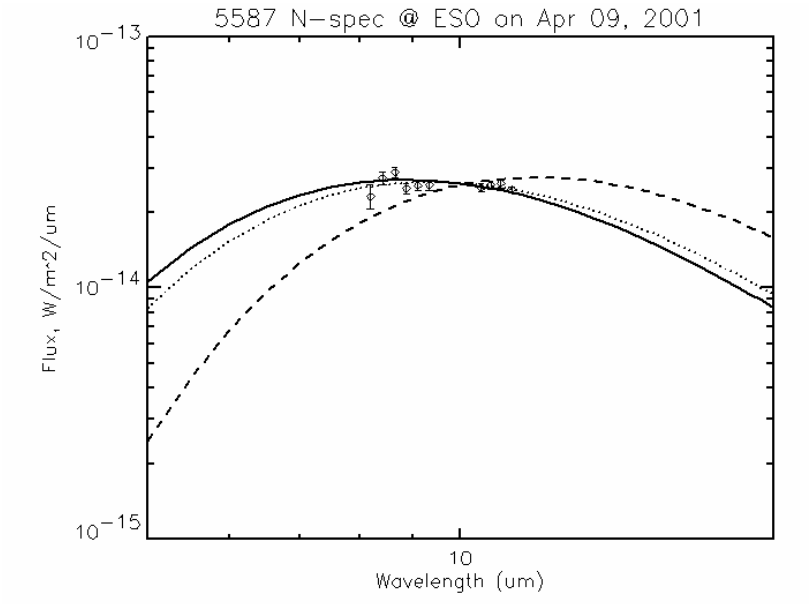

Fig. 4.14 The binned spectrum of the NEA 5587 obtained at 05:46:41 UT on April 09, 2001 (first spectrum) and thermal models fits. Continuous line: STM, dashed line: FRM; dotted line: NEATM.

It is worth pointing out how in the case of Keck observations a severe lightcurve effect had altered the measured spectral energy distribution of the flux, resulting in large scatter of the data points with respect to thermal model continua. Lightcurve correction had proved to reduce dramatically that scatter. However, this might have introduced errors on the derived η-value, diameter and albedo which explain the discrepancy between the Keck and the ESO results.

4.3.10 19356 (1997 GH_3)

This object was observed on April 09, 2001. Thermal infrared data are affected by large uncertainties and the scatter of the data points is large. Unfortunately CCD photometry obtained with the DFOSC at the Danish 1.5m telescope, although of good quality, does not allow the lightcurve amplitude and period to be estimated. Thermal model fits have to rely, therefore, on the uncorrected data. Fits are clearly not as good as in the case where appropriate lightcurve correction could have been performed. Resulting diameter and albedo are listed in Table 4-2.

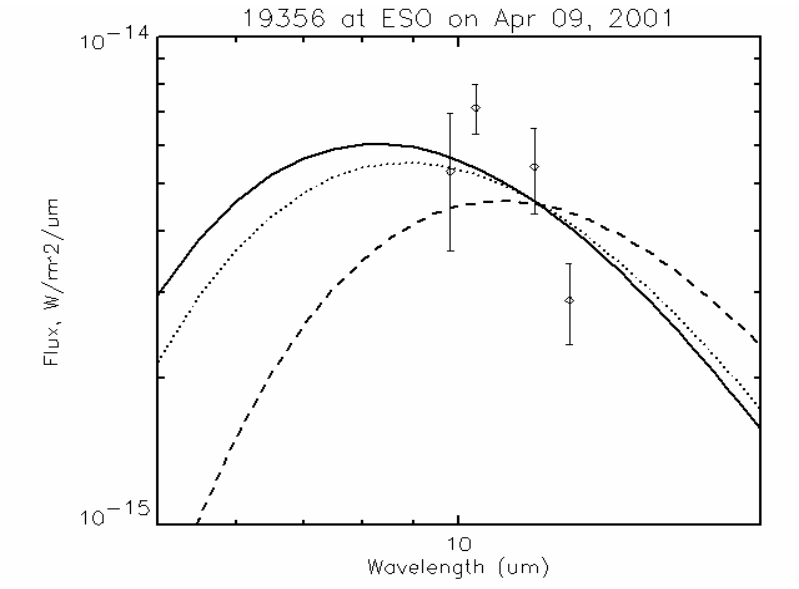

Fig. 4.15 Thermal infrared photometry of the NEA 19356 obtained at ESO and thermal models fits. Continuous line: STM, dashed line: FRM; dotted line: NEATM.

The case of NEA 19356 as well as that of 5587 shows the crucial importance of lightcurve correcting thermal infrared data obtained at different times and the need of simultaneous optical observations.

4.3.11 5604 (1992 FE)

This Aten type NEA was observed at ESO for three nights between April 07 and April 09, 2001. The lightcurve amplitude at that epoch was about 0.2 magnitudes. Absolute calibration of the CCD data was performed. The H magnitude calculated at lightcurve mean is 17.7±0.1, about 1.3 magnitudes fainter than the value given by the Minor Planet Center. This was the weakest source observed within this program (see Appendix A for flux values). Detection was achieved only in the 11.9 μm filter on April 08. However, this result is somewhat questionable since further efforts to image the asteroid in other filters during the same night and again at 11.9 μm on the following nights did not succeed.

Thermal models results are therefore based on this single wavelength measurement. The NEATM derived albedo is lower than the value derived from observations made at Keck on May 2001 (see Delbò et al, 2003) where clear detection was achieved.

4.3.12 37314 (2001QP)

This object was observed on December 02 and December 04, 2001. The V-band lightcurve at the time of the thermal infrared observations indicates a variation within ~0.1 magnitudes. Since two photometric standards were present in the filed of view, absolute calibration was possible. The V magnitude at the time of the thermal infrared observation was found to be equal to 15.6. The H value was calculated using the formulae of Bowell et al (1989) and found to be equal to 14.4 assuming a G value of 0.25, as suggested by Bowell for moderate albedo objects A, B, M, Q or S-types. Derived radiometric albedos and diameter are reported in Table 4-2.

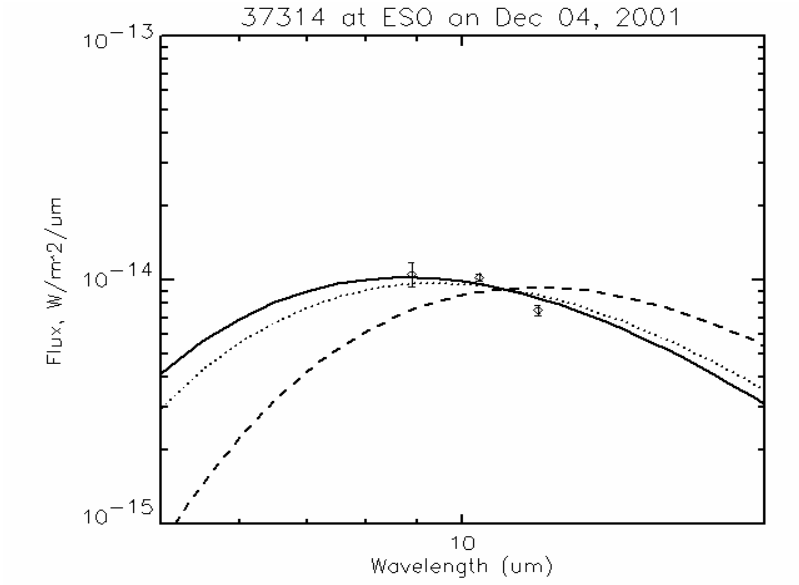

Fig. 4.16 Thermal model fits to N-band infrared data obtained at ESO. Continuous line represents the spectral energy distribution derived by the STM, dashed line that of the FRM and the dotted one is the NEATM.

4.3.13 33342 (1998WT$_{24}$)

CCD observations of this target were carried out from ESO on December 02 and 04, 2001. The lightcurve amplitude was found to be slightly less then 0.2 magnitudes and the absolute calibrated V magnitude at lightcurve mean of 14.63 and 14.23 respectively. The uncertainty of the absolute

calibration is of the order of 0.1 magnitudes. On the basis of the method described by Bowell et al. (1989), I have calculated an H value for 33342 of 18.54±0.1 assuming G=0.4 as expected for this E-type asteroid (Kiselev et al, 2002). The reliability of the H value derived is somewhat questionable given the large phase angle (~60°) at the time of the observations. Thermal infrared data were obtained at 8.9, 10.4 and 11.9 μm and the derived monochromatic flux densities are listed in Appendix A.

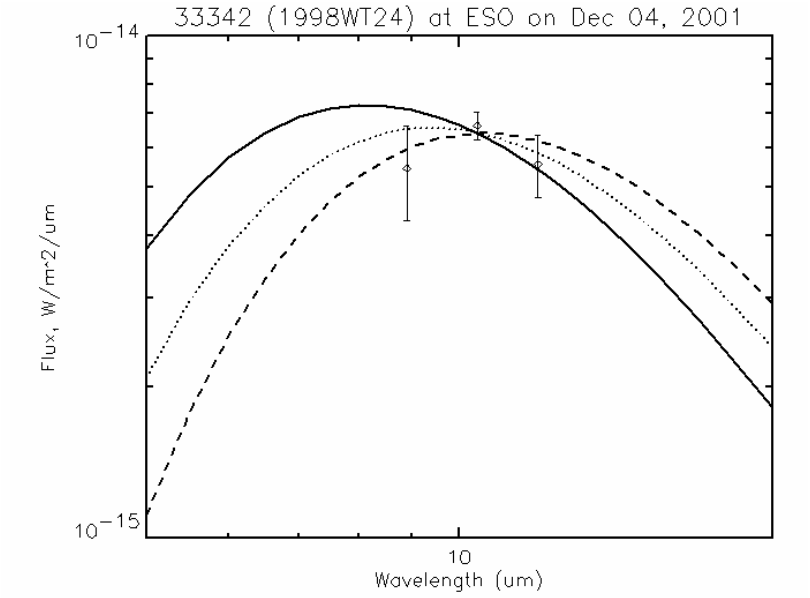

Fig. 4.17 Thermal model fits to N-band infrared data obtained at ESO. Continuous line represents the spectral energy distribution derived by the STM, dashed line that of the FRM and the dotted one is the NEATM.

Resulting radiometric diameter and albedo, from thermal models fit shown in Fig. 4.17, are reported in Table 4-2. NEATM with η fixed to the value of 1.5 gives results which are closer to the radar diameter of Zaitsev et al. (2002) and the polarimetric albedo derived by Kiselev et al. (2002). Fig. 4.17 shows how a smaller η-value, closer to the one assumed by the STM, provide a poor fit to the measured fluxes, indicating that the STM solution is not in agreement with the observations.

Further radiometric observations of this target were obtained with the NASA-IRTF on December 18, 19 and 21, 2001. Fig. 4.18 shows the thermal infrared lightcurve obtained by composing all the 11.7μm-magnitudes of the three nights. A rotational period of 0.15415 days (Pravec, personal communication) was used. Note that the 11.7μm-magnitudes appear to indicate an amplitude of the thermal infrared lightcurve smaller than the optical one. In fact, a sinusoid with period equal to half of the rotation period of the asteroid best fits with an amplitude of 0.18±0.04 magnitudes. However, it is worth to remember that the observing geometry of the target had changed strongly between the three

observing dates at IRTF. This might explain the scatter of the composite thermal lightcurve and might have introduced errors difficult to be estimated. Fig. 4.19 shows thermal model fits to the measured infrared fluxes, which are listed in Appendix A. Lightcurve correcting the observed infrared fluxes in all cases of Fig. 4.19 produces changes of their values no larger then 10%. The shape and the absolute level of the spectral energy distribution resulting from multi-filter photometry are thus not altered significantly. I therefore have applied the thermal models to the uncorrected data increasing their error-bars to about 10% level, where necessary, to account for lightcurve effects.

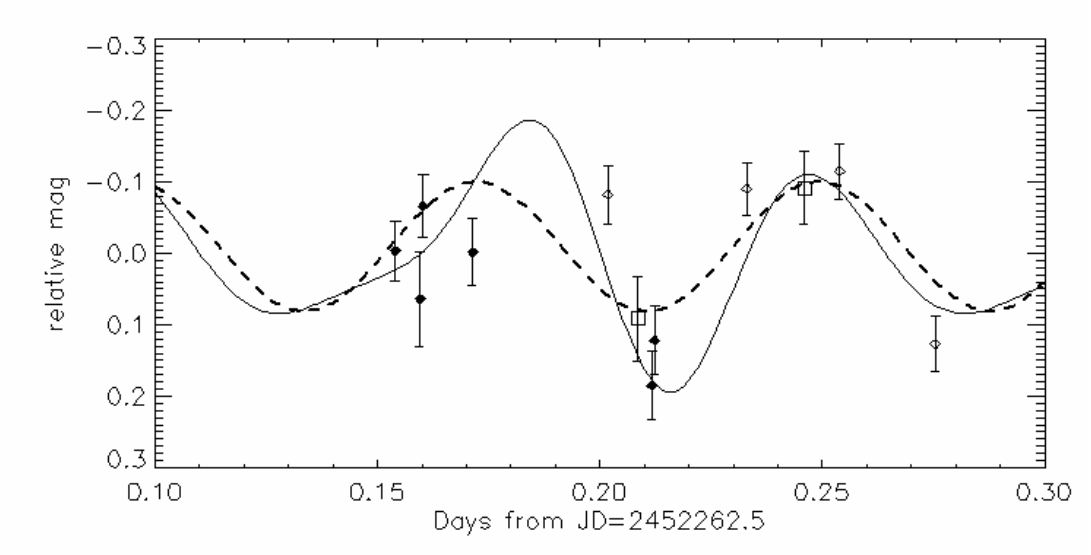

Fig. 4.18 Visible and thermal lightcurve of 33342 on December 2001. Filled diamonds are infrared relative magnitudes derived from 11.7μm-fluxes obtained on December 18, 2001. Empty diamonds represent 11.7μm magnitudes obtained on December 19, 2001 and empty squares those measured on December 21, 2001. Infrared magnitudes were composed on the basis of a 0.15415-days period. Continuous line is the R-band lightcurve derived from CCD observation of Pravec et al. (Pravec, personal communication, 2002). Thick dashed line is a sinusoidal fit with a period equal to half of that of the asteroid to infrared magnitudes.

Resulting diameters and albedos, along with the NEATM fitted η-value are listed in Table 4-3. The spread of the results is very large: the uncertainty on the albedo is almost by a factor of two. The increase of the η-value with the phase angle appears to be real and not the cause of inadequate lightcurve correction or errors in the absolute calibration of the infrared flux. In contrast with the case of 5381 Sekmeth, here, large variations of the η-value correspond to large variations in the resulting diameters and albedos. However, it is worth to point out that observations of the asteroid 33342 were carried out at a different phase angle range with respect to that of the NEA 5381 Sekmeth. The STM fits with a higher albedo, though its value is more stable than the one derived with the NEATM. The FRM appears to give a solution with better agreement with the taxonomic classification for this asteroid,

but it clear that further modeling efforts are in the need to obtain a more realistic explanation for what is going on in this case.

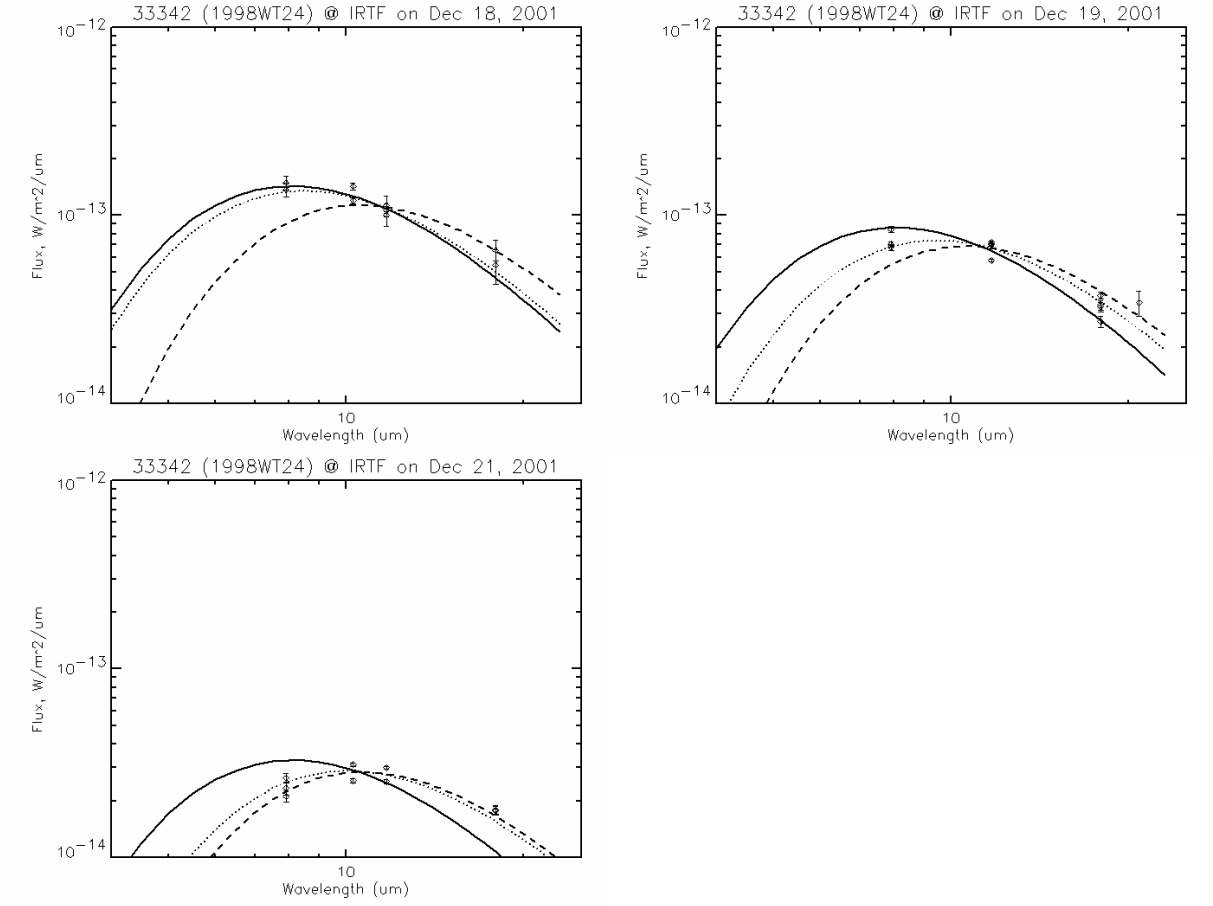

Fig. 4.19 Thermal model fits to multi-filter photometry of the NEA 33342 obtained at the NASA-IRTF. No correction for lightcurve was applied. Continuous line: STM, dashed line: FRM; dotted line: NEATM. Figures are drawn with the same y-axis scale. Note the clear variation of the apparent color temperature between the observing dates.

4.3.14 35396 (1997 XF_{11})

This object is a potentially hazardous asteroid (PHA). It was one of the first asteroids which in early 1998 was predicted to have a small probability of impacting the Earth in 2028. The asteroid was quickly proven safe with more observations and better orbit analysis. It was observed at ESO on November 28, 2002. V band CCD data obtained using the WFI installed at the ESO/MPI 2.2m telescope indicate a lightcurve amplitude not smaller than 0.7 magnitudes. Absolute calibration of the photometry was made observing Landolt's standards at nearly the same airmass of the object and yielded V=15.6±0.1 at mean lightcurve. Assuming G=0.4 as indicated by Bowell et al. (1989) for high albedo objects the resulting H

value was found to be equal to 17.1±0.1. Taking into account the provisional rotational period solution of 3.25730±0.0003 hours (Pravec, 2002)[17] A synthetic lightcurve was fitted to the observational data and the correction factors for the thermal infrared fluxes were derived. In order to account for the rotational variability, thermal infrared fluxes were lightcurve corrected. They are shown in Fig. 4.20 along with thermal models fit continua. Unfortunately, the η value cannot be constrained with sufficient accuracy. The assumption of η=1.0 (phase angle < 45) yields a geometric albedo of 0.4.

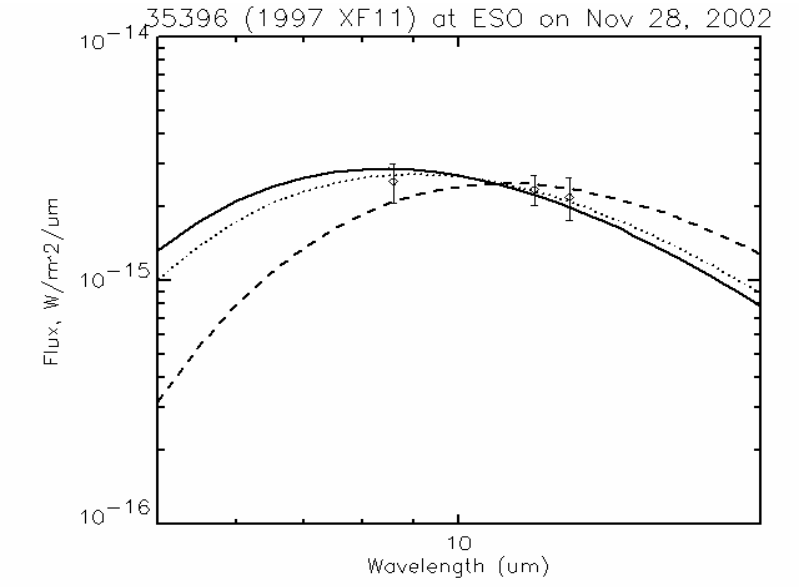

Fig. 4.20 Thermal model fits to the observed flux of the asteroid 35396. Continuous line: STM, dashed line: FRM; dotted line: NEATM.

Further thermal infrared measurements of this object were obtained on November 05 and November 03, 2002 using the MIRSI at the NASA Infrared Telescope Facility (IRTF) on Mauna Kea, Hawaii. Weather conditions were good and the sky transparency of photometric quality (Bus, personal communication). Because of the rapid rotation of the asteroid, several measurements were obtained at 11.7μm to define the thermal lightcurve. Additional measurements defining the spectrum from 4.9 to 18.7μm were interspersed so that the spectral behavior could be determined by interpolation at any point on the lightcurve. The derived monochromatic flux densities at each wavelength and epoch are listed, as usual, in appendix A. The standard star β PEG was used for the reduction of the aperture photometry and observed before and after the target asteroid within about 0.2 airmasses.

[17] MPML Date: Mon Nov 25, 2002 4:42 pm Subject: Re: (35396) 1997 XF11 Lightcurve Observations

In order to construct the thermal infrared lightcurve, the 11.7μm fluxes and their uncertainties were converted to magnitudes[18]. The epoch of measurements were adjusted for light travel time. As described by Harris and Davies (1999), a sinusoidal curve with period equal to half of the sidereal rotational period of 35396 was fitted to the derived relative magnitudes. This curve is shown in Fig. 4.21 with the thin continuous line. The maximum to minimum amplitude of the best fit sinusoid is 0.6±0.07 and 0.5±0.02 magnitudes for the November 05 and November 03 infrared data respectively. Although no simultaneous optical observations were available, Pravec and colleagues obtained a composite V band lightcurve on the basis of observations taken between November 01 and 29. The Pravec et al. lightcurve is superimposed on the thermal one and it is shown in Fig. 4.21 with a dashed thick line. The amplitude of the 11.7μm lightcurve is almost a factor of two smaller than the V band one (The best sinusoidal lightcurve fit yielded an amplitude of 0.92±0.005 magnitudes). Moreover, a phase shift of about 8.5 minutes (i.e. 16°) between the thermal and the visible lightcurve can be measured by comparing the time at which lightcurve minima and maxima occur.

Thermal models fit to the lightcurve corrected fluxes are shown in Fig. 4.22. Note, in both data sets, the very high thermal flux measured at 4.9μm. No explanation for the anomalous results has been found so far. The contribution of the reflected light contributes to the total at 4.9 μm flux. However, such contribution cannot account for the measured high flux.

Taking the mean of the ESO and IRTF results weighted with their uncertainties, the final geometric visible albedo of 35396 is 0.20±0.02 with a diameter of 1.06±0.04. Given the error on the H value estimation of about 10%, the final uncertainties on diameter and albedo result a bit larger.

[18] $m=-2.5\log(F)$; $\sigma m=|2.5/F/ln10\ \sigma F|$

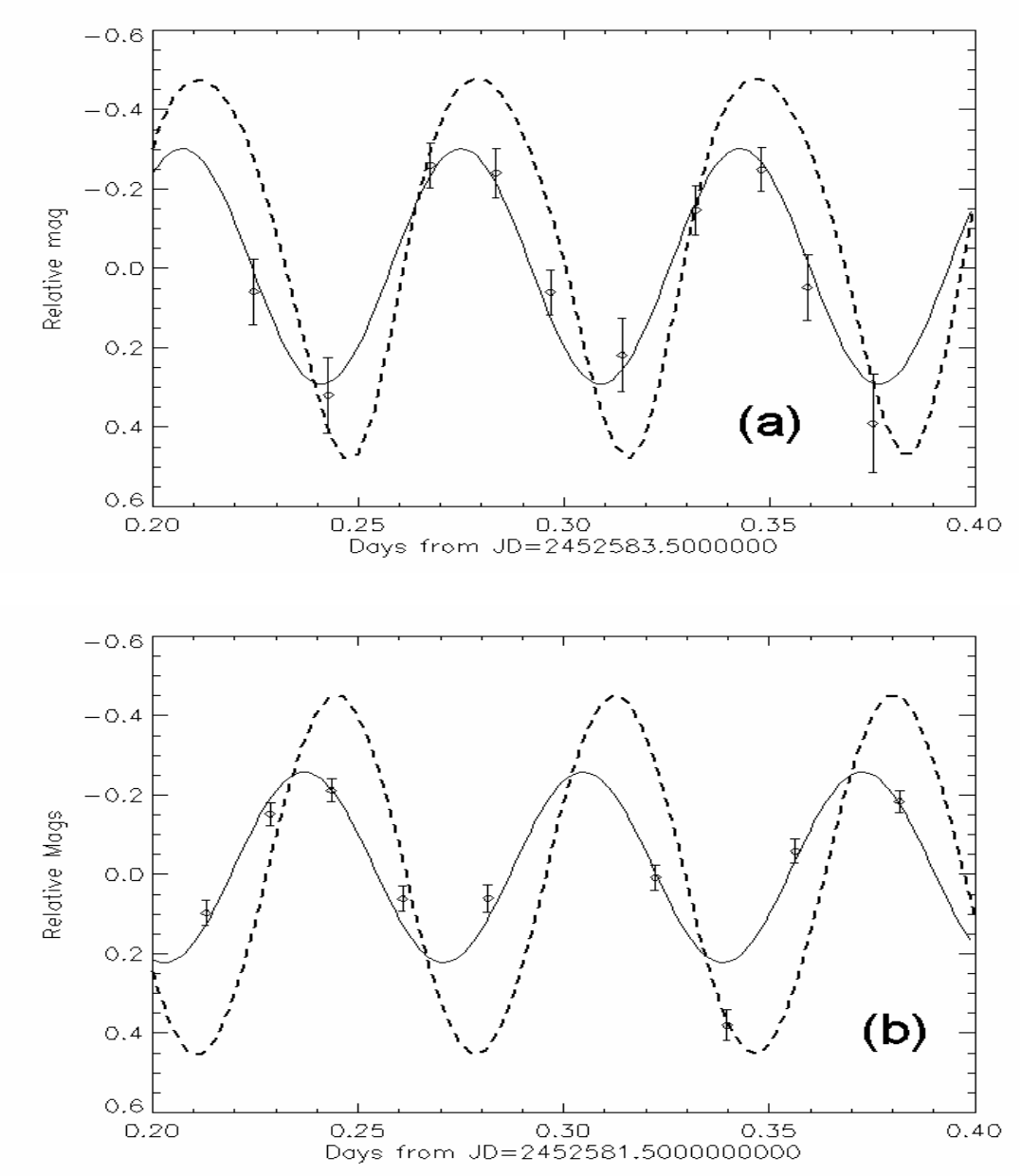

Fig. 4.21 Lightcurve of the NEA 35396 at 11.7μm obtained with MIRSI@NASA-IRTF on November 05, 2002 (a) and on November 03, 2002 (b). The continuous line is a sinusoid function with period half of the rotational period of the asteroid fit to the measured relative magnitudes. The thicker dashed line is the V-band lightcurve of Pravec et al. Note the difference in amplitude and the phase shift.

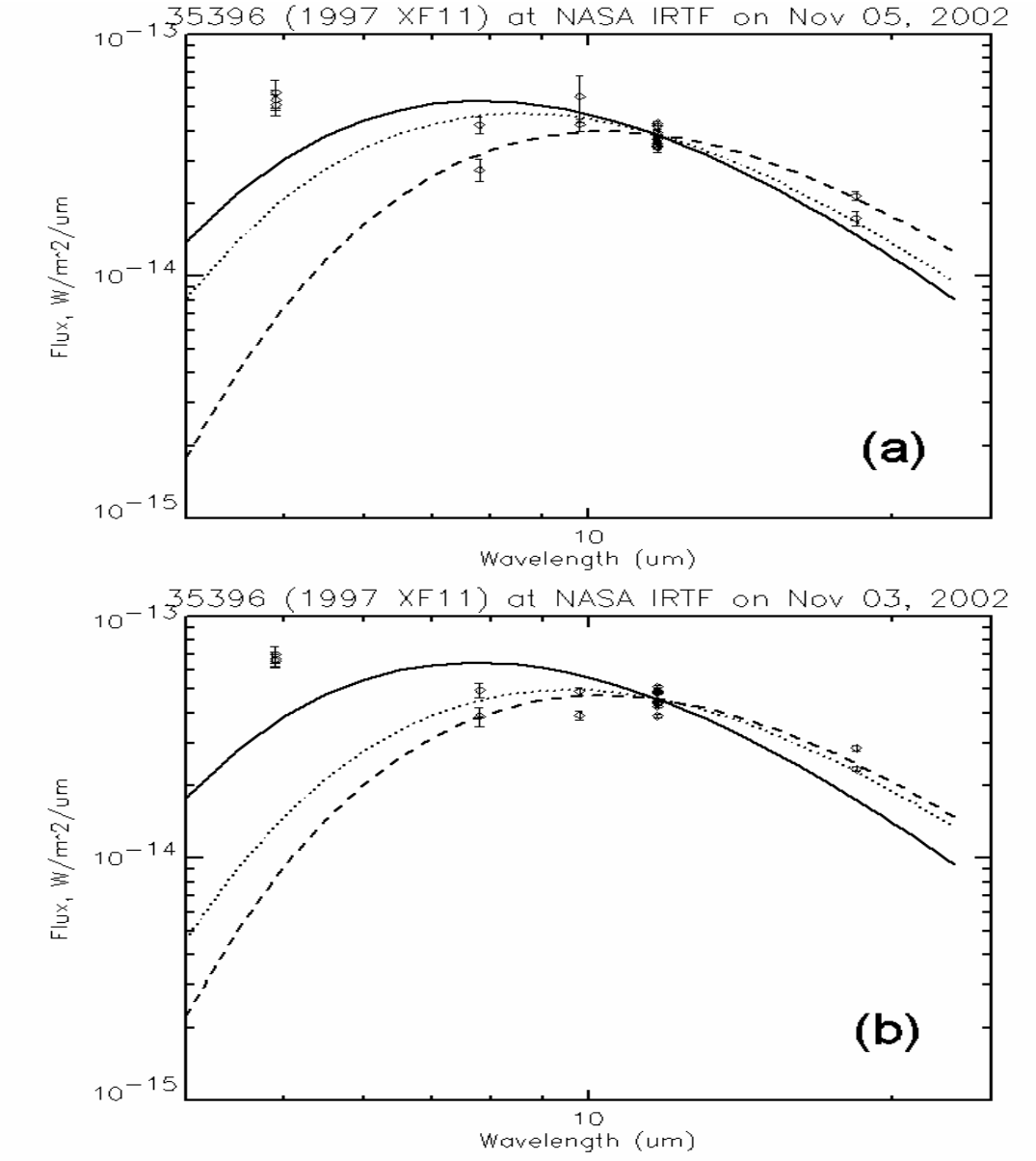

Fig. 4.22 Thermal models fit to the 11.7μm lightcurve-corrected data obtained with MIRSI@NASA-IRTF on November 05, 2002 (a) and on November 03, 2002 (b). Note in both data set the very high thermal flux measured at 4.9μm.

4.3.15 1580 Betulia

Harris (personal communication) analyzed the thermal infrared fluxes obtained at the IRTF on June 02, 2002 and attempted to lightcurve correct them on the basis of the R-band CCD magnitude measured by Yan Fernandez at the 2.2 m University of Hawaii Telescope (Fernandez, personal communication). A 5th-order polynomial was fitted to the R-band magnitudes and used that to

normalize the infrared fluxes to the lightcurve mean. Unfortunately, the R-band lightcurve spans only 2.25 hours of the 6.1-hours-rotational period of this asteroid. The lightcurve mean was estimated by taking the H-value (14.8) from Wisniewski et al. (1997) and calculating the corresponding V magnitude for the geometry of our observations on the basis of the H, G magnitude system. The resulting V-magnitude is 14.12. Assuming V-R = 0.35 for C-type, we get R = 13.77 for the lightcurve mean.

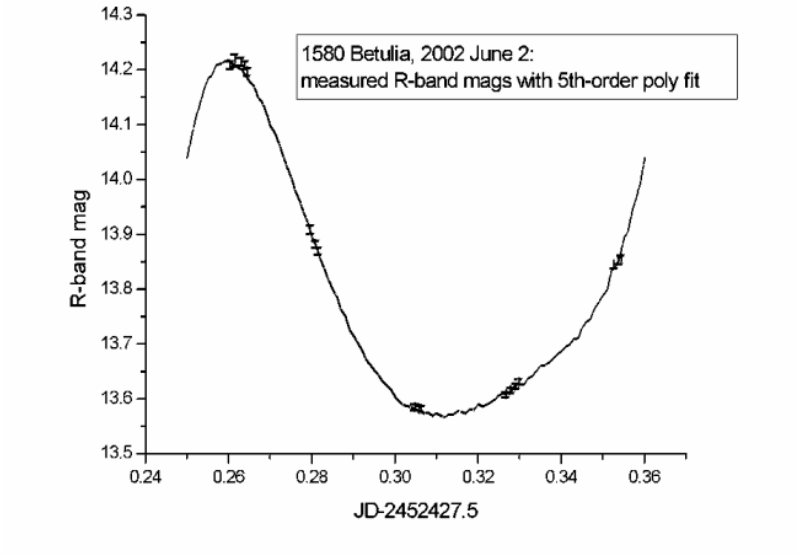

Fig. 4.23 The 5th-order polynomial fitted to the R-band magnitudes measured by Fernandez.

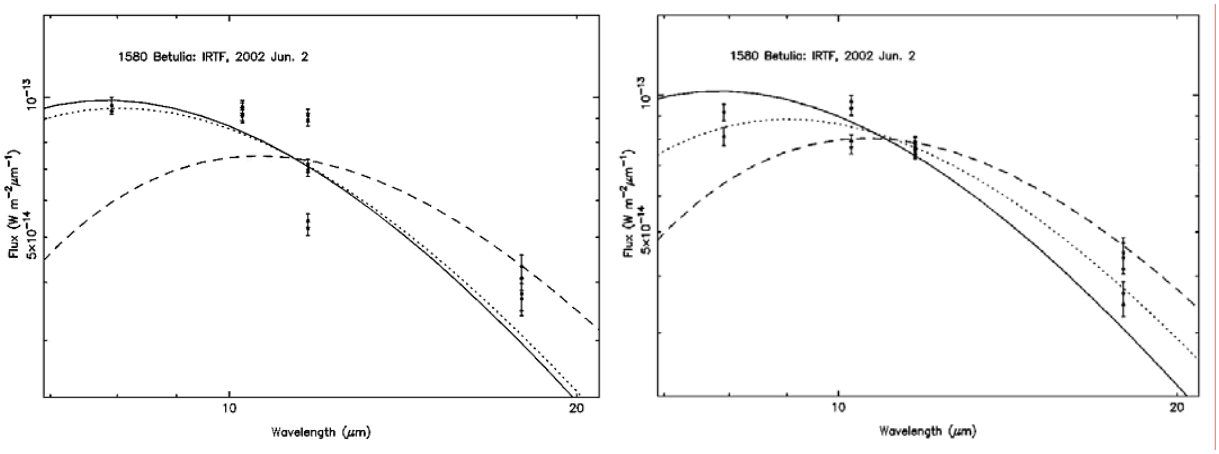

Fig. 4.24 On the left thermal model fits to the observed infrared fluxes before applying lightcurve correction (see text). On the right lightcurve corrected fluxes. Continuous line: STM, dashed line: FRM; dotted line: NEATM.

Harris used the polynomial fit to lightcurve correct thermal infrared fluxes, excluding those taken at times outside the time span of the R-band magnitudes. (5 flux values excluded out of a total of 21). Thermal models were fitted to the data points, first without lightcurve correction (Fig. 4.24 left) and then after lightcurve correction (Fig. 4.24 right). Resulting diameters and albedos are listed in Table 4-5.

STM		**NEATM**			**FRM**	
D (km)	pV	D (km)	pV	η	D (km)	pV
No lightcurve correction						
3.48	0.18	3.38	0.19	0.78	4.89	0.09
With lightcurve correction						
3.54	0.17	4.35	0.11	1.27	5.06	0.08

Table 4-5 Comparison of radiometric derived diameters and albedos on the basis of the three thermal models used in this work. Note the importance of lightcurve correcting the observed thermal infrared fluxes. (see the text for further details)

Pettengill et al. (1979) give a diameter for Betulia of 5.8±0.4 km. However, given the pole solution of Kaasalainen et al. (2004) λ_0=136° and β_0=22° the resulting aspect angle at the time of radar observations was about 88°. The true diameter (i.e. 5.8 × cos(ξ), where ξ is the aspect angle) is therefore very near the radar result. Assuming the dimensional ratios of Kaasalainen et al. (2004), (a/b=1.1 and b/c=1.4) the radar shape of 1580 Betulia is consistent with a tri-axial ellipsoid with semiaxes of 2.9×2.6×1.9 km. The maximum projected area along the line-of-sight was about 15.8 km^2 at the time of radar observations. On the other hand, at the time of the IRTF observations the aspect angle was about 129° and the projected area between 14 and 12.7 km^2 which imply an effective diameter between 4.2 and 4.0 km. Given the uncertainties introduced by lightcurve correcting the observed thermal infrared fluxes and taking into account that the real shape of this asteroid differs significantly from that of a tri-axial ellipsoid (see Kaasalinen et al. 2004), the agreement of radar and NEATM results is good.

The derived albedo is about 0.1. This is consistent with Betulia being a C-type asteroid, but somewhat higher than previous estimates.

4.4 Physical characterization of NEAs: summary of results

We have obtained radiometric diameters and albedos for 32 NEAs. 7 of them where observed under different observing geometries. For 7 objects in our data base the diameter and the albedo had already

been published. However, our new observations have led to a refinement of those values by means of multi-wavelength thermal infrared observations, as in the problematic case of 1580 Betulia.

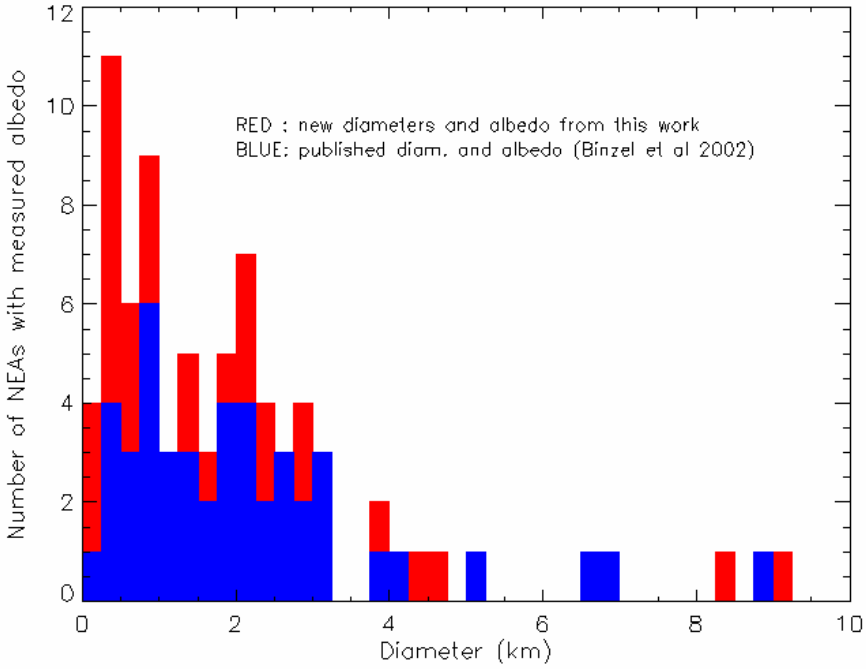

Fig. 4.25 The scientific relevance of this work in terms of newly derived NEA sizes and albedos. The histogram in blue shows the number of NEAs with measured size and albedo as a function of their diameter according to the Table 1 in Binzel et al. (2002) chapter on "Physical Properties of Near-Earth Objects" in Asteroids III. In red are shown new and refined diameters and albedos obtained from this work.

Fig. 4.25 shows the scientific relevance of this work in terms of newly derived NEA sizes and albedos in comparison to what was known before. The histogram in blue color represents the number of NEAs with measured albedo and diameter (as a function of their size) that Binzel et al. (2002) have included in their review paper on the book Asteroids III. In red are shown new and refined diameters and albedos obtained from this work. This work increments the number of NEAs with measured sizes and albedos by 54%. However, if the objects for which we have refined the diameter and the albedo are included, this increment increases to almost 70%.

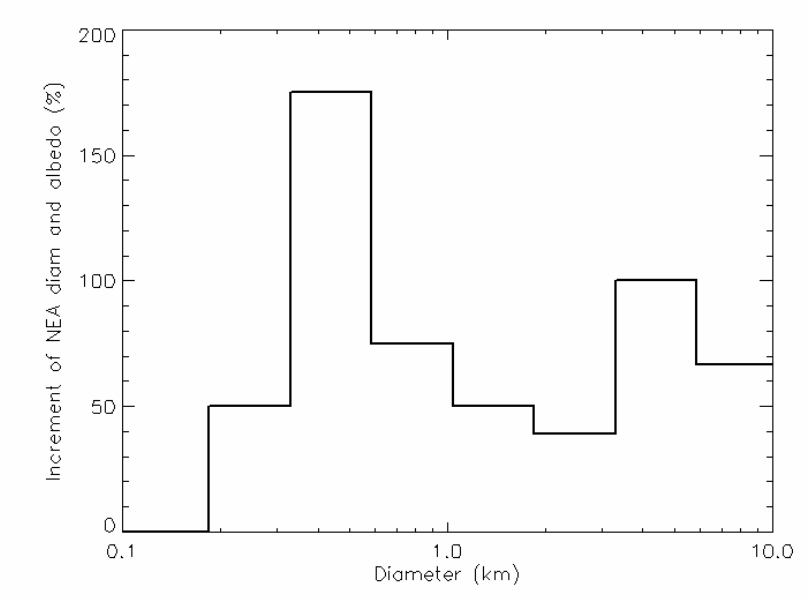

Fig. 4.26 Increment in the number of NEAs with measured diameter and albedo as a function of their diameter. Note how this work contributes manly to the increment of our knowledge for the sub-kilometer population of NEAs.

Fig. 4.26 shows that this work mainly contributed to the physical characterization of object smaller than 1 kilometer. In particular this was possible thanks to the unrivalled sensitivity of the Keck telescope which enabled smaller and fainter objects to be observed, thereby removing the bias inherent in surveys carried out with smaller telescopes that are limited to the largest and brightest objects. The fact that great importance was given to obtain physical information for the sub-kilometer part of the NEA population is important to explore a number of issues of crucial relevance for planetary sciences: are peculiar surface characteristics associated with small asteroids, e.g. lack of space weathering due to the relatively young surfaces of small objects? What are the limitations of asteroid thermal models and what their accuracy for the study of such small objects?

Table 4-6 lists physical parameters for the NEAs studied in this work. Further asteroids with published STM, FRM and NEATM derived sizes and albedos have been included in the list. Taxonomic classes are indicated, where available. Some of the objects were observed under different observing conditions and at different apparitions. Since the solar phase angle is one the most relevant parameter for modeling the thermal emission of asteroids, Table 4-6 reports its value for each observation. Size estimates derived from radar are available for some of the NEAs for which we have obtained radiometric observations. The radar observations put strong constraints on the size and shape of this object thereby providing "ground-truth" data for checking the reliability of the thermal models used.

			NEATM				STM		FRM		Radar		
num	name	α	D	η	pv	ση	D	pv	D	pv	D	pv	Tax
433	Eros (lc max)	10	23.6	1.05	0.20	0.21	20.5	0.27	36.2	0.09	20.06	0.28	S
433	Eros (lc max)	31	23.6	1.07	0.21	0.22	21	0.26	36.6	0.09	20.06	0.28	S
433	Eros (lc min)	10	14.3	1.15	0.22	0.23	11.8	0.32	21	0.1	14.1	0.22	S
1566	Icarus	97	1.27	(1.2)	0.33	-	0.88	0.7	1.05	0.49	1-4	0.09	S
1580	Betulia	12	3.9	(1.2)	0.17	-	3.3	0.24	5.7	0.28	6	0.06	C
1580	Betulia	53	4.35	1.27	0.11	0.3	3.54	0.17	5.06	0.08	6	0.06	C
1620	Geographos	34	2.5	(1.2)	0.26	-	2.2	0.33	3.4	0.14	2.56	0.07	S
1627	Ivar	5	9.12	(1.0)	0.15	-	7.94	0.2	15.9	0.05	8.5±3	0.17	S
1627	Ivar	53	10.2	(1.2)	0.12	-	8.5	0.17	12.6	0.08	8.5±3	0.17	S
1862	Apollo	35	1.4	1.15	0.26	0.23	1.2	0.35	1.9	0.15	1.2	0.38	Q
1685	Toro	18	4.1	(1.2)	0.29	-	3.3	0.44	6.5	0.12	3.3	0.43	S
1866	Sisyphus	16	8.48	(1)	0.15	-	7.47	0.2	16.3	0.042	-	-	S
1866	Sisyphus	35	8.9	1.14	0.14	0.2	7.5	0.2	13.1	0.07		-	S
1915	Quetzalcoatl	29	0.4	(1.2)	0.31	-	0.34	0.42	0.55	0.16	-	-	S
1980	Tezcatlipoca(lcM)	63	6.7	1.54	0.14	0.308	4.5	0.31	6.80	0.14	-	-	Sl
1980	Tezcatlipoca(lcM)	63	6.6	1.64	0.15	0.328	4.5	0.31	6.80	0.14	-	-	Sl
2100	Ra-Shalom	39	2.79	2.32	0.083	0.4	1.6	0.25	2.60	0.095	2.4	0.11	Xc
2100	Ra-Shalom	41	2.5	1.8	0.13	0.36	1.7	0.26	2.60	0.11	2.4	0.11	Xc
2062	Aten	50	0.91	(1.2)	0.28	-	0.77	0.39	1.10	0.18	-	-	S
3200	Phaethon	48	5.1	1.6	0.11	0.32	3.6	0.22	5.50	0.09	-	-	B,F
3554	Amun	16	2.1	1.2	0.17	0.24	1.8	0.23	2.90	0.09	-	-	M
3671	Dionysus	58	1.5	3.1	0.16	0.62	0.86	0.52	1.10	0.31	-	-	Cb
4034	(1986 PA)	40	0.42	(1.0)	0.52	-	0.4	0.58	0.57	0.29	-	-	O
4055	Magellan	13	2.49	(1.0)	0.31	-	2.2	0.39	4.36	0.1	-	-	V
4660	Nereus	60	0.33	(1.5)	0.55	-	0.26	0.86	0.33	0.54	-	-	E
5381	Sekmeth	25	1.3	1.5	0.25	0.2	-	-	-	-	1.05	0.4	S
5381	Sekmeth	29	1.4	1.7	0.24	0.2	1	0.42	1.62	0.17	1.05	0.4	S
5381	Sekmeth	33	1.2	1.3	0.3	0.1	-	-	-	-	1.05	0.4	S
5381	Sekmeth	38	1.4	1.8	0.24	0.2	1	0.45	1.55	0.18	1.05	0.4	S
5381	Sekmeth	42	1.4	1.9	0.22	0.3	-	-	-	-	1.05	0.4	S
5381	Sekmeth	44	1.5	1.9	0.22	0.8	1	0.4	1.50	0.2	1.05	0.4	S
5604	(1992 FE)	18	0.7	(1.0)	0.3	-	0.7	0.3	1.10	0.12	-	-	V
5604	(1992 FE)	36	0.55	(1.0)	0.61	-	0.52	0.69	0.77	0.32	-	-	V
5587	(1990 SB)	19	4	1.1	0.25	0.1	3.4	0.35	6.70	0.09	-	-	Sq
5587	(1990 SB)	42	3.57	0.84	0.32	0.2	3.56	0.51	5.14	0.24	-	-	Sq
5751	Zao	49	2.3	(1.5)	0.36	-	1.8	0.58	2.53	0.29	-	-	E
6178	(1986 DA)	31	2.1	(1.0)	0.17	-	2	0.19	3.05	0.08	-	-	M
6489	Golevka	43	0.33	(1.0)	0.39	-	0.3	0.46	0.47	0.18	0.53	0.15	S
9856	(1991 EE)	36	1	1.15	0.3	0.23	0.85	0.42	1.40	0.16	-	-	S
14402	(1991 DB)	36	0.6	1.04	0.14	0.1	0.56	0.17	0.81	0.08	-	-	C
15817	Lucianotesi	14	0.32	(1.0)	0.64	-	0.3	0.73	0.47	0.29	-	-	E
16834	(1997 WU22)	59	2	(1.5)	0.3	-	1.51	0.53	2.06	0.29	-	-	S
19356	(1997 GH3)	5	0.91	0.98	0.34	0.1	0.83	0.41	1.45	0.13	-	-	S
19356	(1997 GH3)	31	1	(1.0)	0.29	-	0.95	0.3	1.40	0.14	-	-	S
25143	Itokawa	108	0.37	(1.5)	0.19	-	0.2	0.61	0.22	0.54	-	-	S
25330	(1999 KV4)	3	2.55	1.06	0.084	0.17	-	-	-	-	-	-	B

25330	(1999 KV4)	16	2.7	1.3	0.08	0.3	1.26	0.1	4.16	0.03	-	-	B
25330	(1999 KV4)	54	3.21	1.5	0.052	0.2	2.34	0.098	3.41	0.046	-	-	B
33342	(1998 WT24)	60	0.37	(1.5)	0.5	-	0.28	0.84	0.38	0.48	0.41	0.4	E
33342	(1998 WT24)	67	0.34	0.9	0.59	0.1	0.32	0.68	0.40	0.43	0.41	0.4	E
33342	(1998 WT24)	79	0.44	1.5	0.35	0.16	0.32	0.66	0.38	0.48	0.41	0.4	E
33342	(1998 WT24)	93	0.5	1.85	0.27	0.13	0.31	0.77	0.36	0.53	0.41	0.4	E
35396	(1997 XF11)	30	0.89	1.3	0.32	0.8	0.75	0.45	1.16	0.19	-	-	E
35396	(1997 XF11)	53	0.91	1.2	0.31	0.1	0.81	0.39	1.07	0.22	-	-	E
35396	(1997 XF11)	63	1.18	1.8	0.18	0.2	0.83	0.37	1.05	0.23	-	-	E
	1999FK21	35	0.59	0.91	0.32	0.4	0.58	0.33	0.85	0.15	-	-	S
	1999NC43	59	2.22	2.86	0.14	0.5	1.22	0.47	1.62	0.27	-	-	Q
	2000BG19	17	1.77	0.74	0.043	0.2	1.88	0.038	3.25	0.013	-	-	P
	2000EV70	14	0.15	(1.0)	0.6	-	0.14	0.68	0.22	0.29	-	-	Q
	2000PG3	2	4.6	(1.0)	0.042	-	3.9	0.059	8.59	0.012	-	-	D
	2001HW15	11	0.18	(1.0)	0.43	-	0.16	0.54	0.27	0.2	-	-	-
	2001FY	22	0.32	(1.0)	0.52	-	0.3	0.59	0.48	0.23	-	-	S
	2001LF	45	2	1.4	0.05	0.1	1.5	0.08	2.50	0.03	-	-	C
	2002AV4	70	1.5	1.6	0.37	0.25	1.1	0.73	1.40	0.43	-	-	-
	2002BM26	60	0.84	3.1	0.023	0.4	0.41	0.094	0.57	0.05	-	-	P
	2002CT46	23	0.16	(1.0)	0.32	-	0.15	0.36	0.24	0.15	-	-	Sr
	2002QE15	50	1.49	(1.5)	0.24	-	1.15	0.4	1.63	0.2	-	-	S

Table 4-6 Radiometric diameter and albedos, compared with the one derived from radar observations.

If not otherwise stated, radiometric diameters and albedos are from this work. Other original data sources: (**433**), (**1980**), (**3671**): see Harris and Davies, (1999); (**1862**), (**3200**), (**3554**): see Harris, (1998); (**2100**), (**9856**): Harris et al., (1998). For (**3671**) we have taken the NEATM solution requiring $\eta = 3.1$ (see Harris and Davies, 1999). The FRM also provides a reasonable fit to the data for (**3671**), but it gives a much higher albedo of 0.30–0.35, which is seriously inconsistent with the taxonomic type of Bus and Binzel (2002).

Taxonomic classes are from Bus and Binzel (2002) and from Binzel et al. (2002) with the exceptions of (**4055**) Magellan (Cruikshank et al., 1991) and (**4660**) Nereus (Binzel et al., 2004).

For **433 Eros** results, given for lightcurve maximum and minimum, are from Harris and Lagerros (2002). The albedo from *NEAR Shoemaker* is 0.25 ± 0.06 (Veverka et al., 2000). Lightcurve effects have been taken into account where corresponding optical photometry is available; in all other cases included.

Radar diameter sources: (**1566**), (**1580**), (**1627**), (**1862**), (**2100**), (**6178**), (**6489**): Harris and Lagerros, (2002); (1620) Equivalent spherical diameter from shape model, Hudson and Ostro (1999); (**5381**): Nolan et al. (2003); (**33342**): Zaitsev et al. (2002). However, Di Martino et al. (2004) give indication of a larger diameter ~ 0.6km. (**1685**) Ostro et al., (1983).

Other radar diameters at: http://echo.jpl.nasa.gov/~lance/asteroid_radar_properties/nea.radaralbedo.html